AD-A051 735 NAVAL ACADEMY ANNAPOLIS MD DIV OF ENGINEERING AND WEAPONS F/G 21/7
THE NAVAL ACADEMY HEAT BALANCED ENGINE (NAHBE). (U)
JUN 76 R BLASER, B RANKIN, A POURING
UNCLASSIFIED USNA-EW-8-76 NL

| OF |
AD
A051735

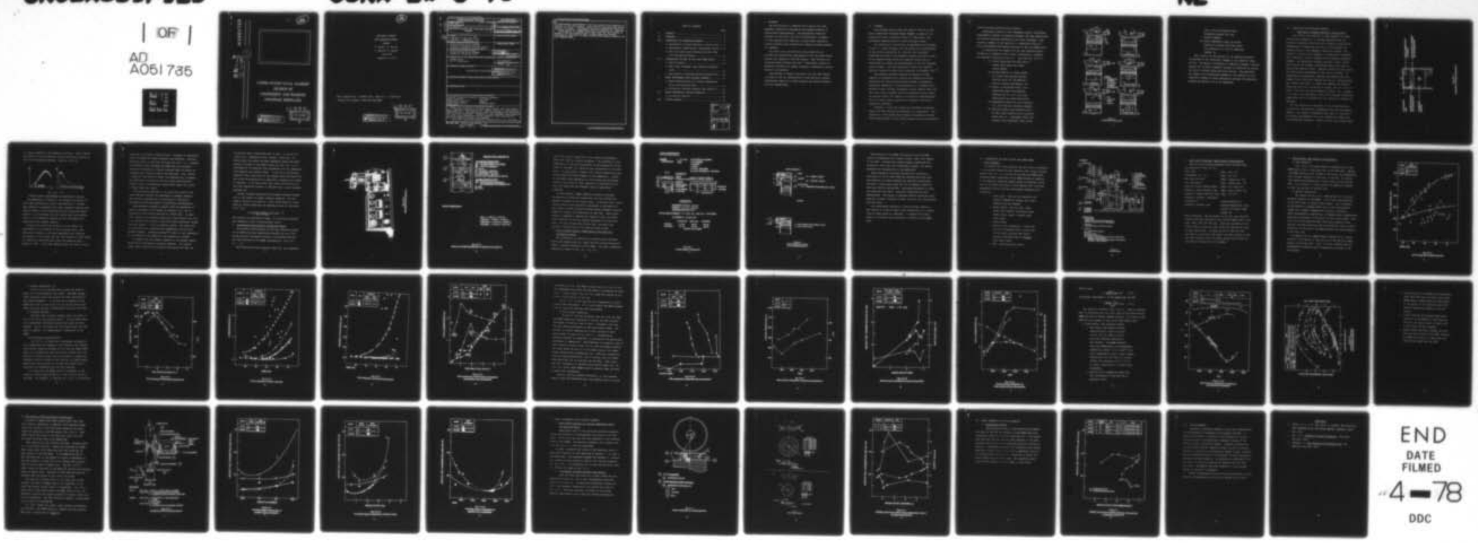

END
DATE
FILMED
4-78
DDC

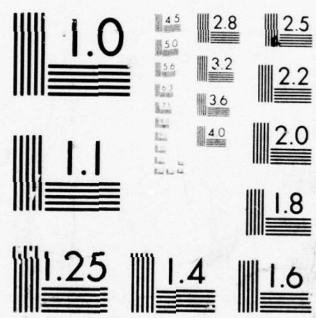

MICROCOPY RESOLUTION TEST CHART

NATIONAL BUREAU OF STANDARDS-1963-A

26

UNITED STATES NAVAL ACADEMY
DIVISION OF ENGINEERING AND WEAPONS
ANNAPOLIS, MARYLAND

(26)

THE NAVAL ACADEMY

HEAT BALANCED ENGINE*

(NAHBE)

R. Blaser, A. Pouring

E. Keating, B. Rankin

June 1976

Report E. W. 8-76

*Work Supported by: NAVSEA 0331F, under Dr. F. Ventriglio through work request N 000 2476 WR 62250

SECURITY CLASSIFICATION OF THIS PAGE (When Data Entered)

REPORT DOCUMENTATION PAGE		READ INSTRUCTIONS BEFORE COMPLETING FORM
1. REPORT NUMBER USNA-EW-8-76	2. GOVT ACCESSION NO.	3. RECIPIENT'S CATALOG NUMBER
4. TITLE (and Subtitle) The Naval Academy Heat Balanced Engine (NAHBE).		5. TYPE OF REPORT & PERIOD COVERED Progress rept. Apr-June 76
		6. PERFORMING ORG. REPORT NUMBER
7. AUTHOR(s) R. Blaser, A. Pouring, B. Rankin, E. Keating		8. CONTRACT OR GRANT NUMBER(s)
9. PERFORMING ORGANIZATION NAME AND ADDRESS United States Naval Academy Division of Engineering and Weapons Aerospace Engineering Department		10. PROGRAM ELEMENT, PROJECT, TASK AREA & WORK UNIT NUMBERS
11. CONTROLLING OFFICE NAME AND ADDRESS United States Naval Academy Annapolis, Maryland 21402		12. REPORT DATE June 1976
		13. NUMBER OF PAGES 51 53p.
14. MONITORING AGENCY NAME & ADDRESS (if different from Controlling Office) NAVSEA 0331F Dr. F. Ventriglio		15. SECURITY CLASS. (of this report) Unclassified
		15a. DECLASSIFICATION/DOWNGRADING SCHEDULE N/A

16. DISTRIBUTION STATEMENT (of this Report)

Distribution Unlimited

DISTRIBUTION STATEMENT A
Approved for public release;
Distribution Unlimited

17. DISTRIBUTION STATEMENT (of the abstract entered in Block 20, if different from Report)

18. SUPPLEMENTARY NOTES

19. KEY WORDS (Continue on reverse side if necessary and identify by block number)

Internal Combustion Engines
Spark Ignition
Compression Ignition
Multi-Fuel Engine
Combustion
Pressure Exchange
Pollution
Energy
Combined cycle

20. ABSTRACT (Continue on reverse side if necessary and identify by block number)

The heat balanced or combined cycle engine with time dependent combustion sustained by two chamber geometry is demonstrated experimentally. The theoretical basis and hardware for achieving the cycle are described. Evidence of time dependent heat addition is given where combustion creates pressure waves sustained by pressure exchange between two chambers.

The basic cycle and operating characteristics are reviewed

DD FORM 1 JAN 73 1473 EDITION OF 1 NOV 65 IS OBSOLETE
S/N 0102-014-6601

406 923 JOB

SECURITY CLASSIFICATION OF THIS PAGE (When Data Entered)

20.

and experimental performance of CFR and glass-walled engines are compared to the OTTO engine. Open throttle and throttled engine results are given. Preliminary results on parametric variation of engine variables, compression ignition behavior are reported.

Improvements in thermal efficiency over the OTTO engine in excess of 45% are demonstrated in some operating regimes. Considerable reduction in peak pressure and exhaust emission are also demonstrated.

TABLE OF CONTENTS

I. ABSTRACT

The heat balanced or combined cycle engine with time dependent combustion sustained by two chamber geometry is demonstrated experimentally. The theoretical basis and hardware for achieving the cycle are described. Evidence of time dependent heat addition is given where combustion creates pressure waves sustained by pressure exchange between two chambers.

The basic cycle and operating characteristics are reviewed and experimental performance of CFR and glass-walled engines are compared to the OTTO engine. Open throttle and throttled engine results are given. Preliminary results on parametric variation of engine variables, compression ignition behavior are reported.

Improvements in thermal efficiency over the OTTO engine in excess of 45% are demonstrated in some operating regimes. Considerable reduction in peak pressure and exhaust emission are also demonstrated.

II. FOREWORD

This progress report gives the state of the art of the Naval Academy Heat Balanced Engine (NAHBE) in terms of its theoretical basis, laboratory tests of a CFR engine, and preliminary demonstration of a multi-cylinder engine.

The resources of the Division of Engineering and Weapons of the U. S. Naval Academy, the new theoretical understanding of the process proposed by Dr. Pouring, the invaluable experience and help of the Technical Support Division as well as the Computer Aided Design and Graphics Group have all contributed to further the understanding of the heat balanced engine concept. Its early theoretical basis and proposed practical application were first presented in November 1974.[1]

The pressure exchange interaction between cylinder chambers as proposed by Dr. Pouring has supplied governing parameters for this non-equilibrium process of combustion. Laboratory comparison of the performance of a standard and a modified single cylinder transparent engine (Megatec Mark III) has given visual evidence that this nonsteady process cannot be analyzed within the domains of equilibrium thermodynamics and the classic energy equations for chemical reactions of combustion processes.

Moreover, a 1938 (AD) L-Head four cylinder Continental engine has been modified and operated in a dynamometer. The simplicity of the modification support the expectation that future applications of this novel process will allow production within existing manufacturing processes.

Preliminary results in the transparent engine, preliminary experimental evidence of pressure exchange, and some observations on the multi-cylinder modification are first discussed. Then follows a summary of the results of a comparative test of a fully instrumented CFR engine operating in OTTO and NAHBE modes.

To familiarize the reader with the heat balanced engine concept as it appears to the current investigators, consider the sequence of events in Fig II-1. (See also Fig. III-1.1).

(1) Piston approached top dead center, intake valve opens and intake stroke begins.

(2) Initial portion of intake stroke air enters the cylinder through auxilary inlet (D) followed by a fuel-air charge from venturi (E).

(3) Charge is stratified with a rich composition above the pressure exchange cap (C) and a very lean composition just above the piston.

(4) Compression forces air into reservoir (B), also known as balancing chamber.

(5) Ignition causes rapid pressure build up with large pressure ratio occurring across gap (C). Subsequent shock compression wave propagates under piston

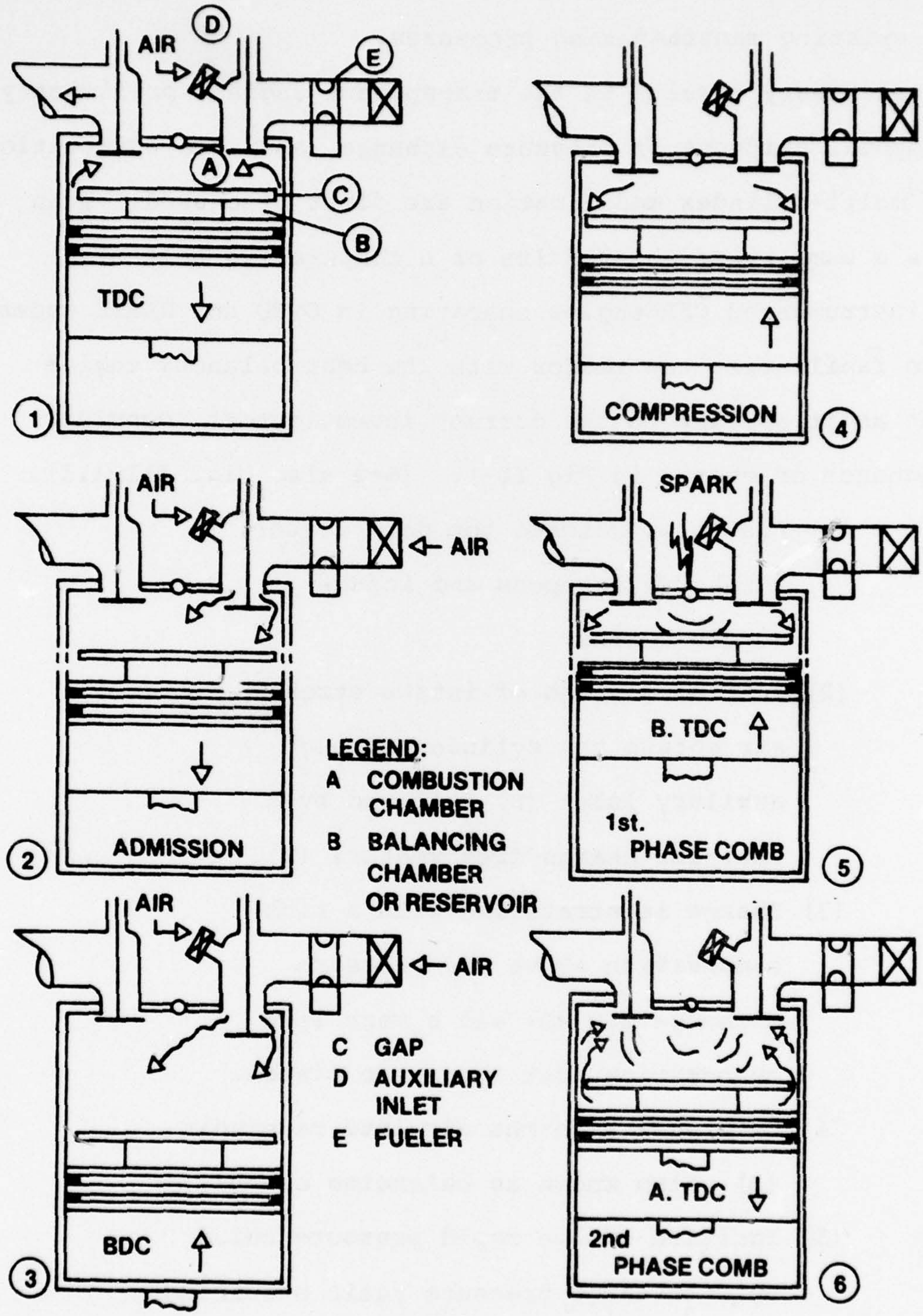

Fig. II-1.1
Heat Balanced Engine Cycle

piston cap with expansion wave propagating upward into combustion chamber.

(6) Shock compression under cap builds pressure to higher value than above cap causing air to flow to combustion chamber (A).

Thus, control of the pressure in the combustion process is achieved by the "balancing" chamber or air reservoir under the cap. The degree of balancing of combustion between "constant volume" and "constant pressure" process is controlled by varying the ratio of volumes above and below the cap. The additional air pumped from the balancing chamber or air reservoir to the combustion chamber by shock compression prolongs the combustion process and allows it to go to completion.

III. COMBUSTION WITH PRESSURE EXCHANGE

1. Experimental Pressure Behavior, Previous Work

The criteria for selecting a given geometry for demonstrating the feasibility of the Heat Balanced Cycle was originally determined from the basic concepts of equilibrium thermodynamics considering the flow of gases between two chambers during a time dependent combustion process. The reason for selecting two chambers, a primary and a secondary, was to provide a "relief" chamber for the primary combustion chamber. The geometries proposed initially, holes, valves and cavities (for example, perforated piston caps) did not achieve the expected result. Material failure and heat transfer difficulties contributed to this lack of success. By broadening the experimental approach and assuming that the chamber could interaction through the use of a narrow annular gap (rather than holes), a simple new geometry was adopted which gave the first indication of success (see Fig. III-1.1). After a few trial and error dimension changes, (eg., Volumes A. B, gap C) the experimental data fully confirmed theoretical expectation and p-v diagrams much like those for a diesel was obtained.

For the analysis and evaluation of the characteristics of the cycle, piezoelectric transducers were used as pressure sensors. Two separate transducers were used for recording a pv diagram and expanded view of the combustion process with its related peak pressure. During the test well defined peaks

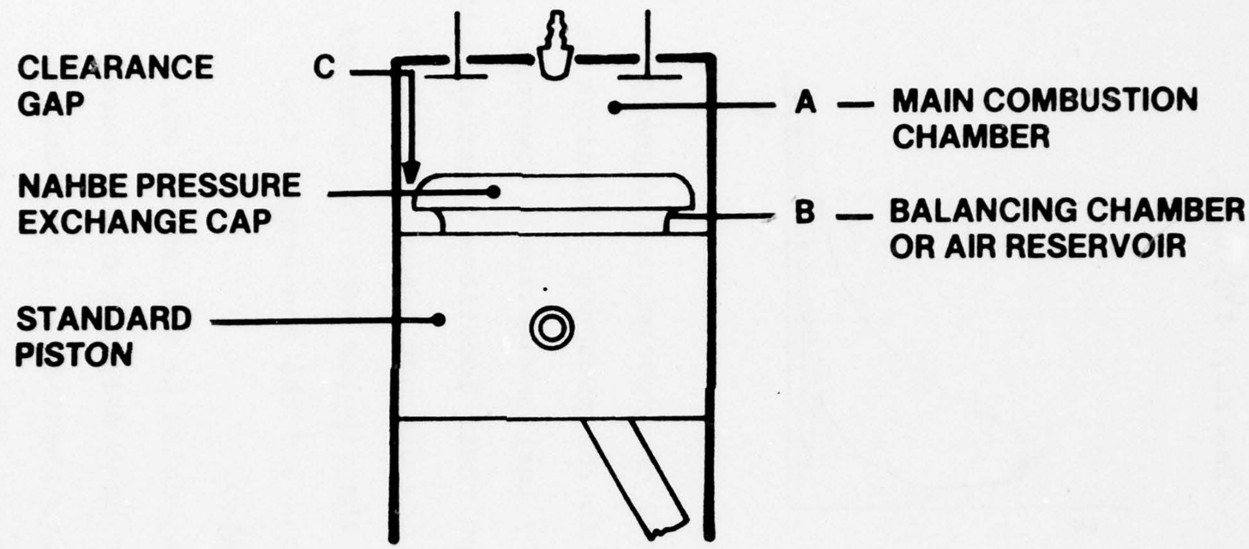

Fig. III-1.1
Schematic of engine geometry

or ripples appeared in the pressure recording. These covered the period of all the addition of heat from spark ignition to part of the expansion process. (See Fig. III-1.2)

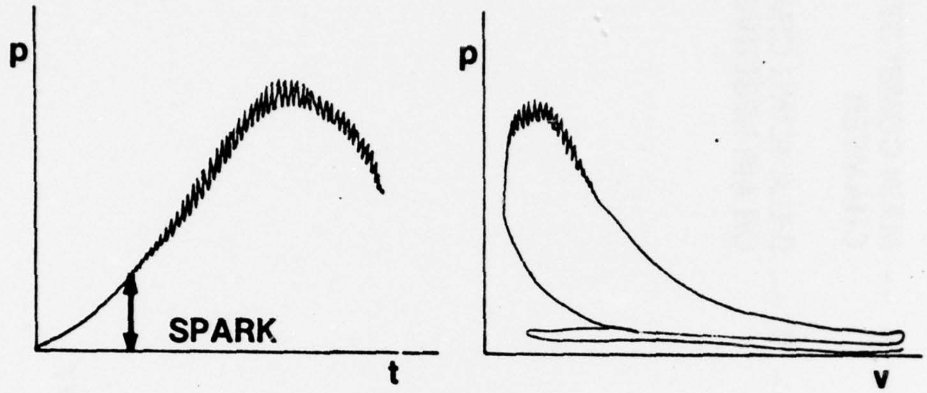

Fig. III - 1.2

Pressure peaks superimposed on experimental signals

The appearance of ripples in the pressure recordings at first were attributed to faulty instrumentation. However, when changes of transducers and their locations together with careful checks of the electronics did not change the ripple pattern, it was accepted that the ripples were the combined result of the combustion process and the non-steady flow generated by the chamber geometry.

Although the prevailing objective at the moment was achievement of the combined or heat balanced cycle, some exploratory analysis of the wave phenomenon was conducted. For example, it was noted that the time duration of each ripple or indentation was practically equal and remained equal change of load. It has been observed that the overall ripple amplitude is related to engine output. Increase of compression ratio increases the ripple frequency and amplitude. Defining balancing ratio or the ratio of V_B/V_A, Fig. III - 1.1, increase in balancing ratio decreases the amplitude and frequency. Increase or decrease in annular clearance does not effect the frequency but inversely affects the amplitude. And, finally a change of fuel does not affect the frequency but it appears the amplitude is related to the fuel flash characteristic. Alcohol gives a low amplitude ripple while diesel fuel gives a higher amplitude ripple.

The preliminary analysis of the wave-like nature of the ripple pattern reflects its dependency on chamber geometry, and indicates improbability of developing a theoretical explanation within the domain of equilibrium thermodynamics.

The mechanism proposed to explain this new phenomemon is based on concepts of non-steady gas dynamics (2,3) and is analogous to the process observed in a shock tube. In shock tube, rupture of a diaphram supporting a high pressure gas from a low pressure gas creates a shock wave which propagates through the tube compressing the low pressure medium. The shock wave is sustained by an expansion wave propagating into the high pressure medium. Pressure exchange[2] refers to the compression of one medium at the expense of the expansion of another.

It appears that the ripples observed in the present experiments can be attributed to pressure exchange. The ripples appear when a solid cap is placed on the piston yet they are not present when a perforated disk is used. It can be concluded that a compression wave, perhaps a shock wave, is driven under the piston cap when combustion causes the rapid pressure increase in the upper volume (V_A, Fig. III - 1.1). Coincidently, an expansion wave propagates into the combustion zone dropping the pressure there. If the cap is perforated, immediate short circuiting of the pressure above and below the cap occurs and essentially no reduction of pressure nor ripple is observed. It is shown later that nearly 50% reduction in the peak combustion pressure is possible with a solid pressure exchange cap.

Further evidence supporting the pressure exchange concept lies in the number of cycles (ripples) observed. For the chamber length on the order of 1 inch, sound speed is on the order of 25,000 inches/sec and combustion lasts on the order of 10^{-3} sec.

$$n \cong \frac{25{,}000 \text{ inches} \times 10^{-3} \text{ sec}}{\text{sec} \times 1 \text{ inch}} = 25$$

This matches the approximate number of oscillations observed per combustion stroke in oscilloscope traces.

2. Experimental Observations, Transparent Engine

The unusual characteristics of the heat addition process of the NAHBE have been demonstrated through the use of two single-cylinder transparent engines, one standard OTTO and the other modified to the NAHBE configuration. (Fig. III - 2.1, - 2.2.

Both engines have been operated under the same conditions

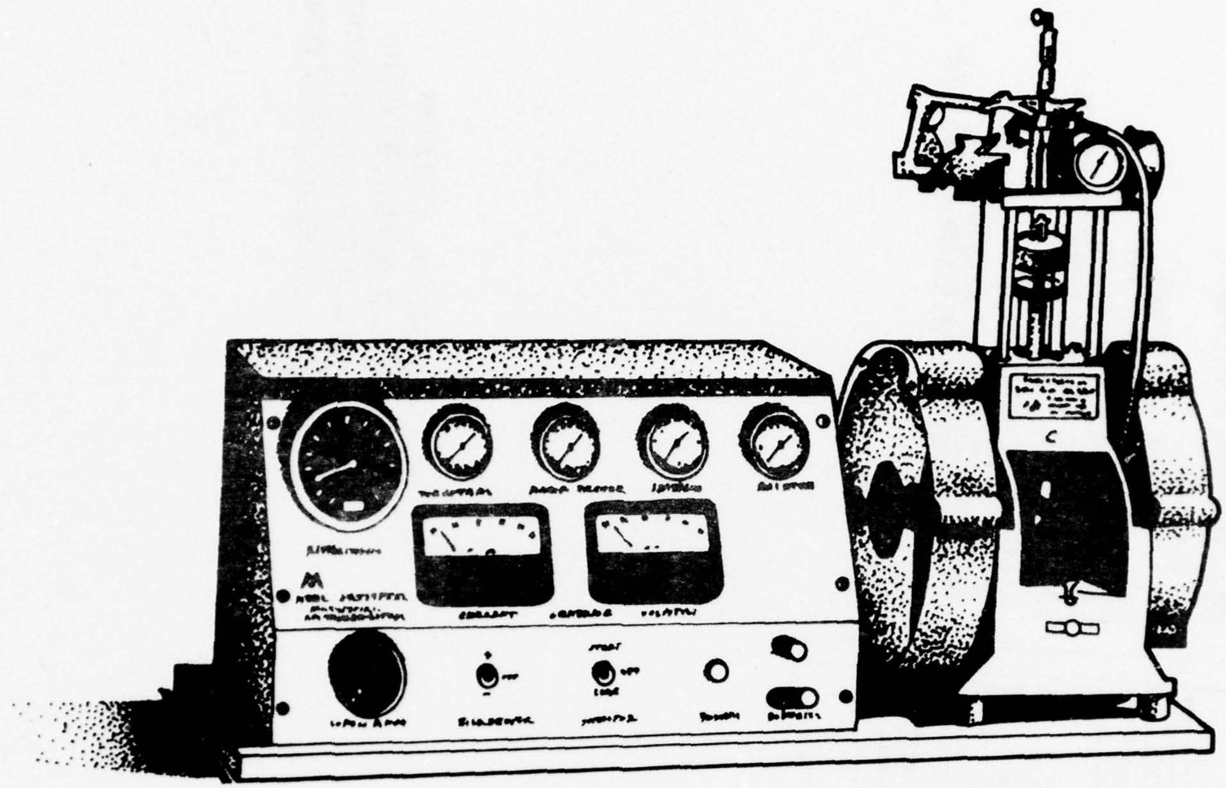

Fig. III-2.1
THE MEGATECH MARK III

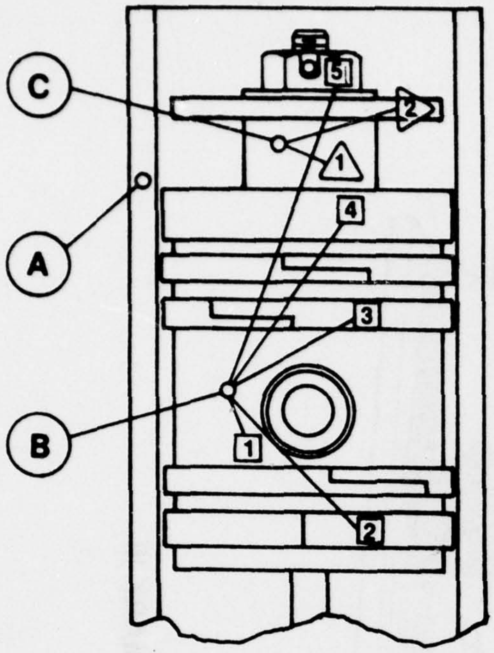

MEGATECH MARK III

STANDARD OPERATION

Ⓐ— TRANSPARENT CYLINDER

Ⓑ— PISTON ASSEMBLY

1 PISTON
2 LOW GUIDE — GRAPHITE
3 COMPRESSION RING ASSY
4 UPPER GUIDE — GRAPHITE
5 BOLT, NUT, WASHER AND COTTER PIN

NAHBE MODIFICATION

Ⓒ— PISTON HEAD ASSEMBLY
OR PRESSURE EXCHANGE CAP

1 RING
2 PLATE

BASIC DIMENSIONS

DIA. — 1.625 in., 4.127 cm
STROKE — 2.000 in., 5.08 cm
SURFACE — 2.074 in^2, 13.38 cm^3
VOLUME — 4.148 in^3, 16.97 cm^3

Fig. III-2.2
Details of NAHBE Modification to MEGATECH MARK III

and direct visual comparison of the combustion phenomenon shows that they are totally different. The influence of the composition of the fuel air mixture on the propagation of the flame in the media as a whole is very pronounced for the OTTO cycle. At best power, a white, very intense combustion propagates through the whole chamber at the composition. Orange is the basic color appearing in rich mixture and the characteristic blue color of total combustion is obtained only at very low loads with the attendant lack of operational stability.

On the contrary, NAHBE combustion reflects excellent progression of molecular dissociation and the influence of pressure exchange at all engine loads. At maximum load a white central zone of fast molecular interaction is enclosed by a blue layer in which pressure exchange between chambers supplies oxygen for ending the dissociation of the fuel. When engine output is reduced by reducing the supply of fuel, the white zone decreases in size but remains enclosed in a large blue zone. At very low load with little fuel, the white zone becomes a central point in an otherwise blue volume.

3. Multi-cylinder Engine - Modification 1938 Jeep Y112 Continental Engine

The feasibility of converting an existing multi-cylinder engine was demonstrated on a spark ignition L-head Continental engine, standard equipment in 1938 Jeeps. The basic components effected are shown in Fig. III - 3.1, 3.2.

BASIC COMPONENTS

ENGINE (STANDARD)	Y - 4112 (SI) **TYPE**	CONTINENTAL ENGINE
		4 CYLINDERS
		4 STROKE
		L HEAD
		41 HP AT 3300 RPM
		84 FOOT POUNDS AT 1500 RPM

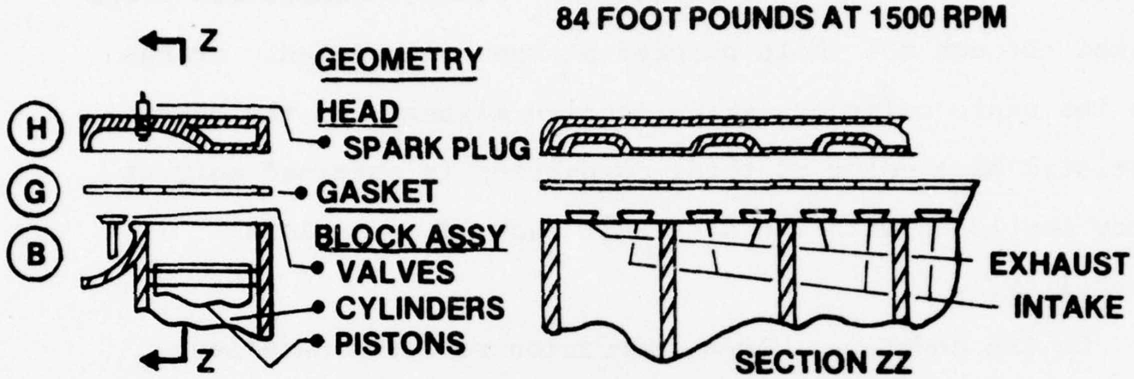

DIMENSIONS

DIAMETER 3-3/16 in., 8.10 cm
STROKE — 3-1/2 in., 8.89 cm
COMPRESSION RATIO 6:1

TOTAL DISPLACEMENT—111.7 CU. IN.—1831 CC = 1.83 LITERS

CYLINDER V = 27.92 CU IN.

	VALVE DIA	SEAT DIA	OPENING
INTAKE	1.20 IN.	1.06 IN.	.291 IN.
EXHAUST	1.01 IN.	.875 IN.	.292 IN.

SPARK PLUG 18MM.

Fig. III-3.1
L-Head Engine Components

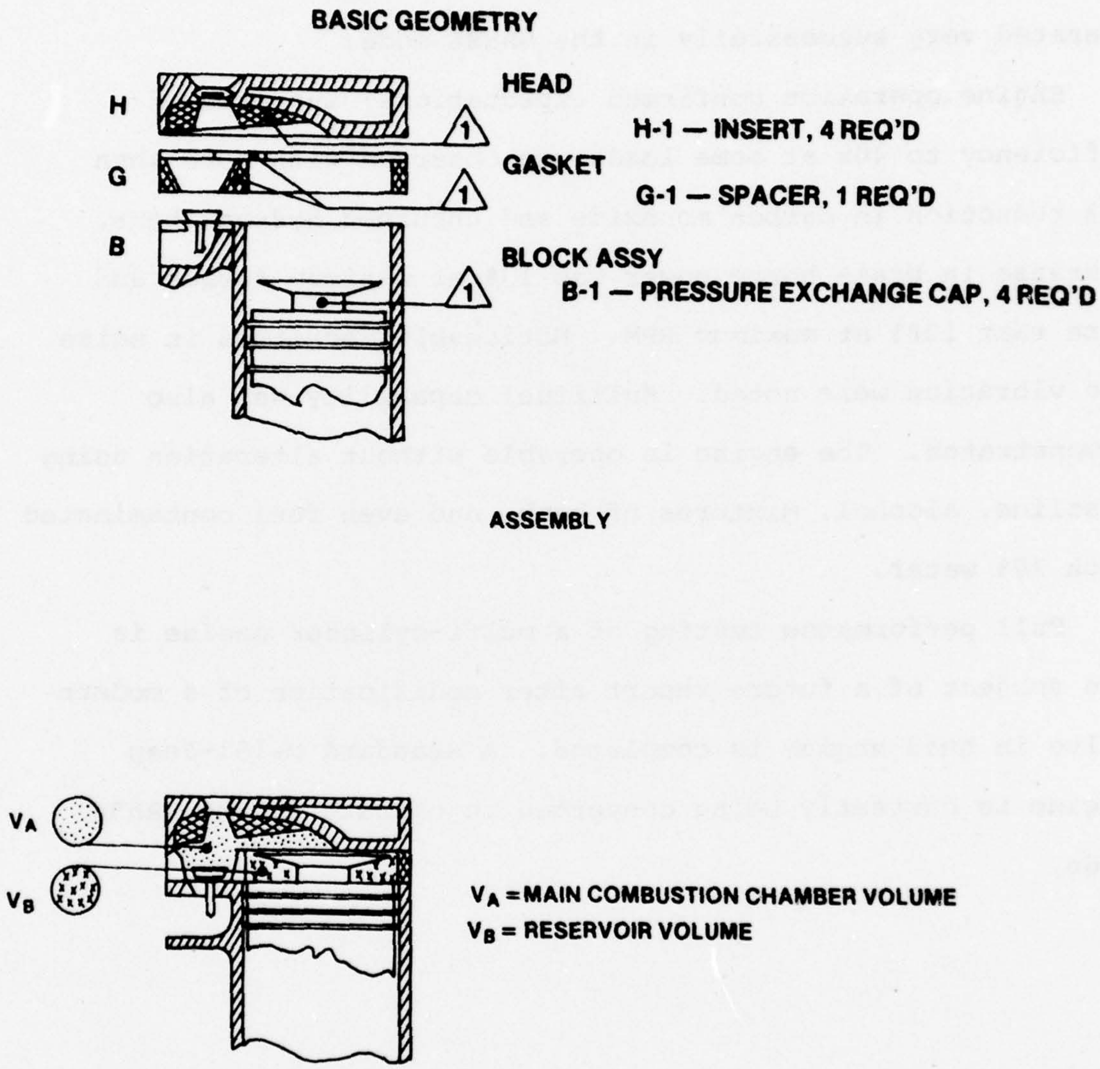

Fig. III-3.2
Engine modification required for the heat balanced cycle.

Modification to the NAHBE configuration was performed without disassembling the original engine, other than removal of the head. Although the L-head geometry complicated the conversion, after few trial dimensional changes, the engine operated very successfully in the NAHBE mode.

Engine operation confirmed expectations; increase of efficiency to 40% at some loads was observed with more than 80% reduction in carbon monoxide and unburned hydrocarbons. Increase in brake horse power was 15% at maximum torque and more that 100% at maximum RPM. Noticeable decreases in noise and vibration were noted. Multifuel capability was also demonstrated. The engine is operable without alteration using gasoline, alcohol, mixtures of both, and even fuel contaminated with 20% water.

Full performance testing of a multi-cylinder engine is the subject of a future report after modification of a modern valve in head engine is completed. A standard M-151-Jeep engine is currently being converted to operate in the NAHBE mode.

IV. COMPARATIVE CFR TEST OF OTTO AND NAHBE MODES

1. Test Variables

To confirm and further amplify the data cited in reference 1, an existing Combustion Fuel Research (CFR) single cylinder engine, Fig. IV - 1.1, was run in the OTTO and NAHBE modes. Although direct comparison of the NAHBE should be conducted in the sense of comparing engines based on different cycles such as the OTTO and Diesel, it was decided that five basic parameters could be used for performance comparison and evaluation:

- Fuel cycle: This can be related to the mixture composition because the intake geometry was not changed.
- Total output: THP (or IHP), where brake plus internal frictional output equals total output, assuming equal heat losses.
- Brake output
- Specific fuel consumption: Using fuel per total horsepower hour, noting that in the single cylinder CFR engine internal frictional work is <u>greater</u> than brake output.
- RPM: Revolutions per minute

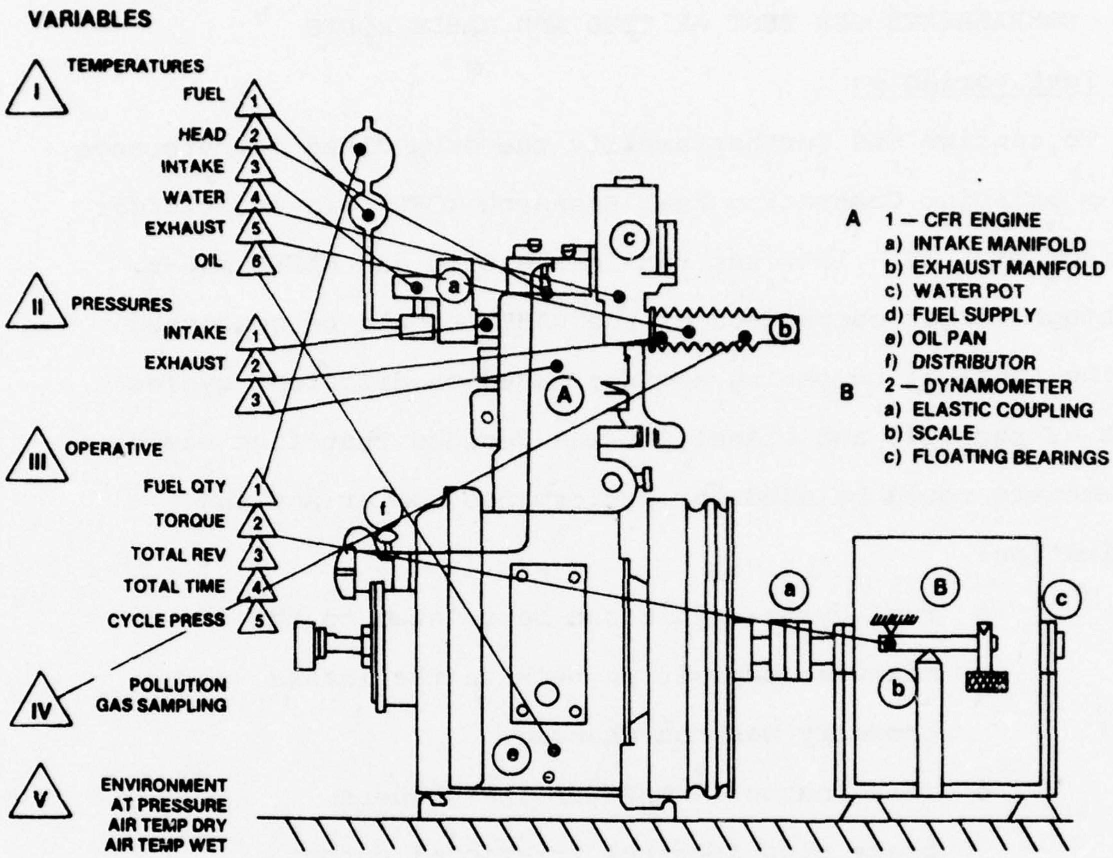

INSTRUMENTATION

I TEMPERATURES
SENSOR—IRON CONSTANTAN THERMOCOUPLES
READOUT—SOLID STATE DIGITAL THERMOMETER

II PRESSURES
SENSOR AND READOUT—MERCURY COLUMNS

III OPERATIVE
1 CALIBRATED CONTAINER 50cc
2 SCALE
3 PULSE COUNTER
4 ELECTRICAL STOPWATCH
5 SENSOR—QUARTZ TRANSDUCER WITH SIGNAL CONDITIONER
POSITION — ANGULAR SIGNAL
READING — OSCILLOSCOPE FOR DIAGRAM AND PEAK PRESSURE
RECORDING — PEAK PRESSURES

Fig. IV-1.1
CFR engine details

2. Basic Test Procedures, Open Throttle Configuration

Data for the following parameters were recorded using the apparatus of Fig. IV.-2.1.

Fuel level	Temp., fuel (°C)
Dynamometer (ft. lb.)	Temp., air (°C)
Run time (for 50cc)	Temp., intake man. (°C)
Run revolutions	Temp., exhaust man. (°C)
Ignition timing (degrees BTDC)	Temp., cyl. head (°C)
Pressure, intake manifold (Hq)	Temp., water jacket (°C)
Pressure, exhaust manifold (psi)	Temp., oil (°C)
Pressure, cylinder, continuous recording of	Carbon Monoxide (%)
Pressure, cylinder (psi)	Unburned Hydrocarbon (ppm)
	Oxides of Nitrogen (ppm)
	Oxygen (%)

Test procedures: The CFR engine in its full open throttle configuration was operated in the OTTO and NAHBE mode at 900, 1100, 1200, 1300 and 1500 rpm. Data were recorded at five output loads at each rpm cited within the operational range of each engine mode. A second series of tests was also performed by optimizing the engines for best economy at each rpm, both fuel/air ratio and spark advance were varied for the OTTO and timing only in the NAHBE.

3. Test Results, Open Throttle Configuration

a) Peak pressure:

Fig. lV-3.1, the peak pressure at maximum load of the NAHBE mode is 40% or less than that of the OTTO mode. Because the NAHBE maintains high volumetric efficiency and subsequently high cylinder pressure at the point of ignition, the engine also operates satisfactorily at lower loads and rpm than the OTTO. As is shown in a later section the NAHBE will operate at very low rpm with or without load.

b) Exhaust temperature:

The results of Fig. IV-3.2 demonstrate one of the outstanding features of the NAHBE. A well known characteristic of the OTTO leads to exhaust valve damage: this is because, as the mixture is reduced below that of the stoichiometric composition, exhaust temperatures continue to increase. Below stoichiometric composition, the NAHBE exhaust temperatures decrease continuously as the amount of fuel is decreased. Moreover, this curve shows the basic operating regimes of both engines, the OTTO operating from stoichiometric (about 5.8×10^{-5} lbs/cycle) to rich while the NAHBE operates from stoichiometric to the very lean.

It appears that the NAHBE exhaust temperature is related directly to the amount of fuel and not to the fuel/air composistion as with the OTTO. This, in effect, demonstrates the fundamentally different mode of combustion occurring in the two engines.

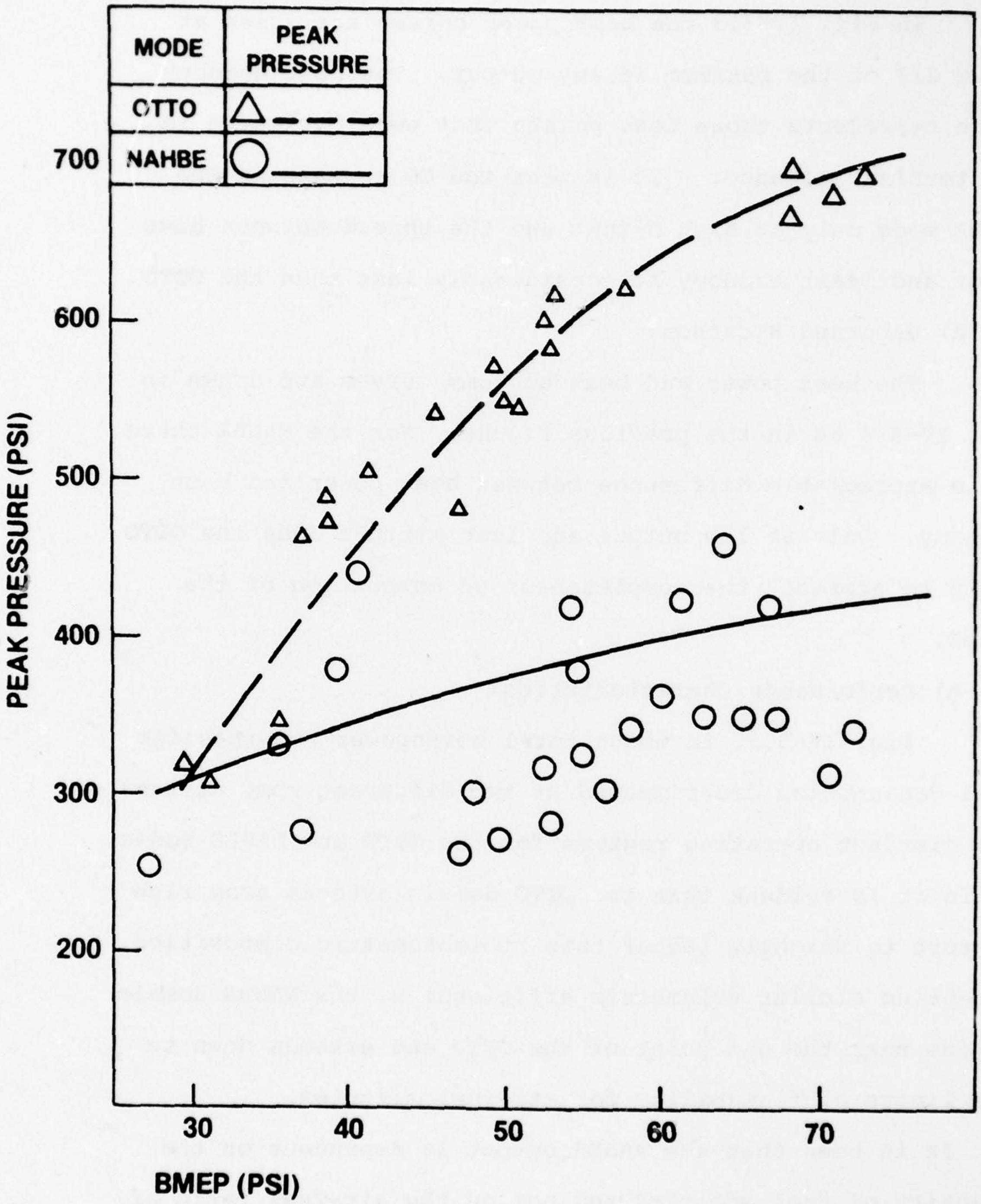

Fig. IV-3.1
CFR comparison of peak pressures

c) Exhaust Emmissions, CO:

In Fig. IV-3.3 the best power curves are drawn at about 2/3 of the maximum at any output. The best economy curve represents those test points that were optimized in the testing sequence. It is seen the CO appears in the NAHBE mode only at high output and the spread between best power and least economy is considerably less than the OTTO.

d) Unburned Hycarbon:

The best power and best economy curves are drawn in Fig. IV-3.4 as in the previous figure. For the NAHBE there is no appreciable difference between best power and best economy. Only at low output and lean mixture does the OTTO begin to approach the completeness of combustion of the NAHBE.

e) Performance Characteristics:

Fig. IV-3.5, in which total horsepower and specific fuel consumption are compared at two different rpm, defines the distinct operating regimes for the OTTO and NAHBE modes. Again it is evident that the OTTO domain extends from rich mixture to slightly leaner than stoichiometric composition. Accepting similar volumetric efficiencies, the NAHBE domain begins near the end point of the OTTO and extends down to the limits of flamability for air-fuel mixtures.

It is seen that the NAHBE output is dependent on the quantity of fuel admitted and not on the air-fuel ratio of the OTTO. For example, at 1500 rpm for a total (or indicated)

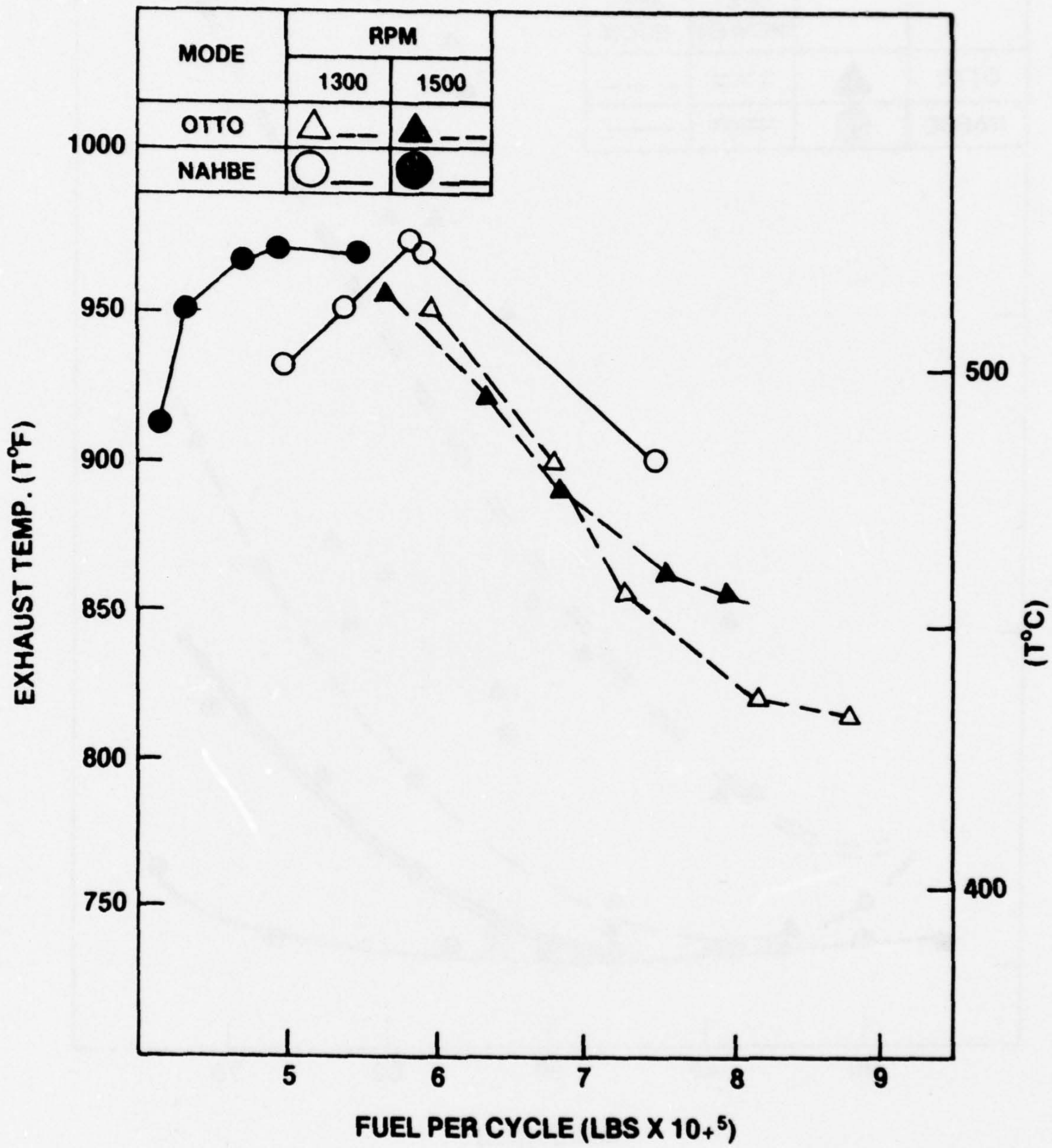

Fig. IV-3.2
CFR comparison of exhaust gas temperatures

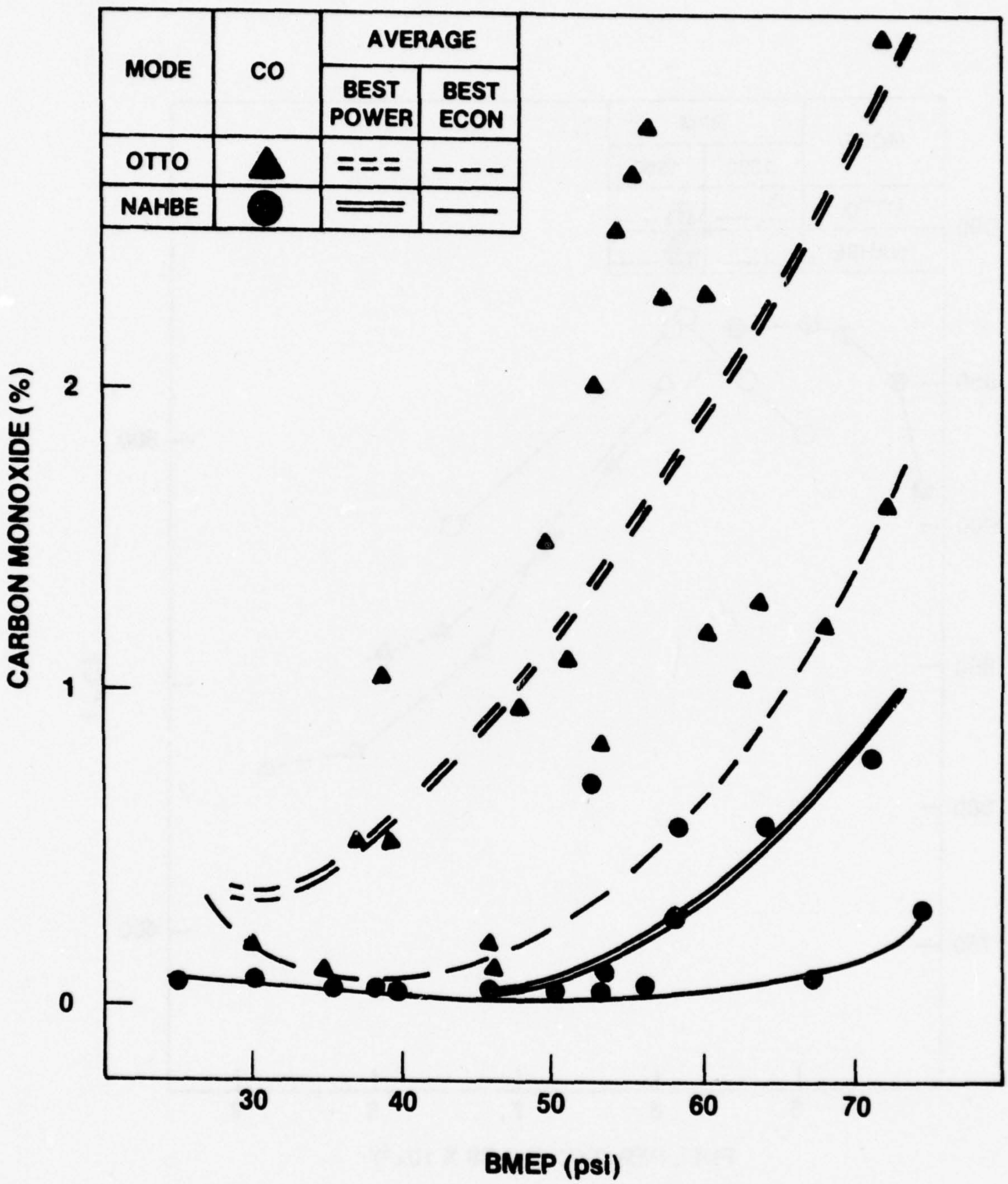

Fig. IV-3.3
CFR comparison of carbon monoxide

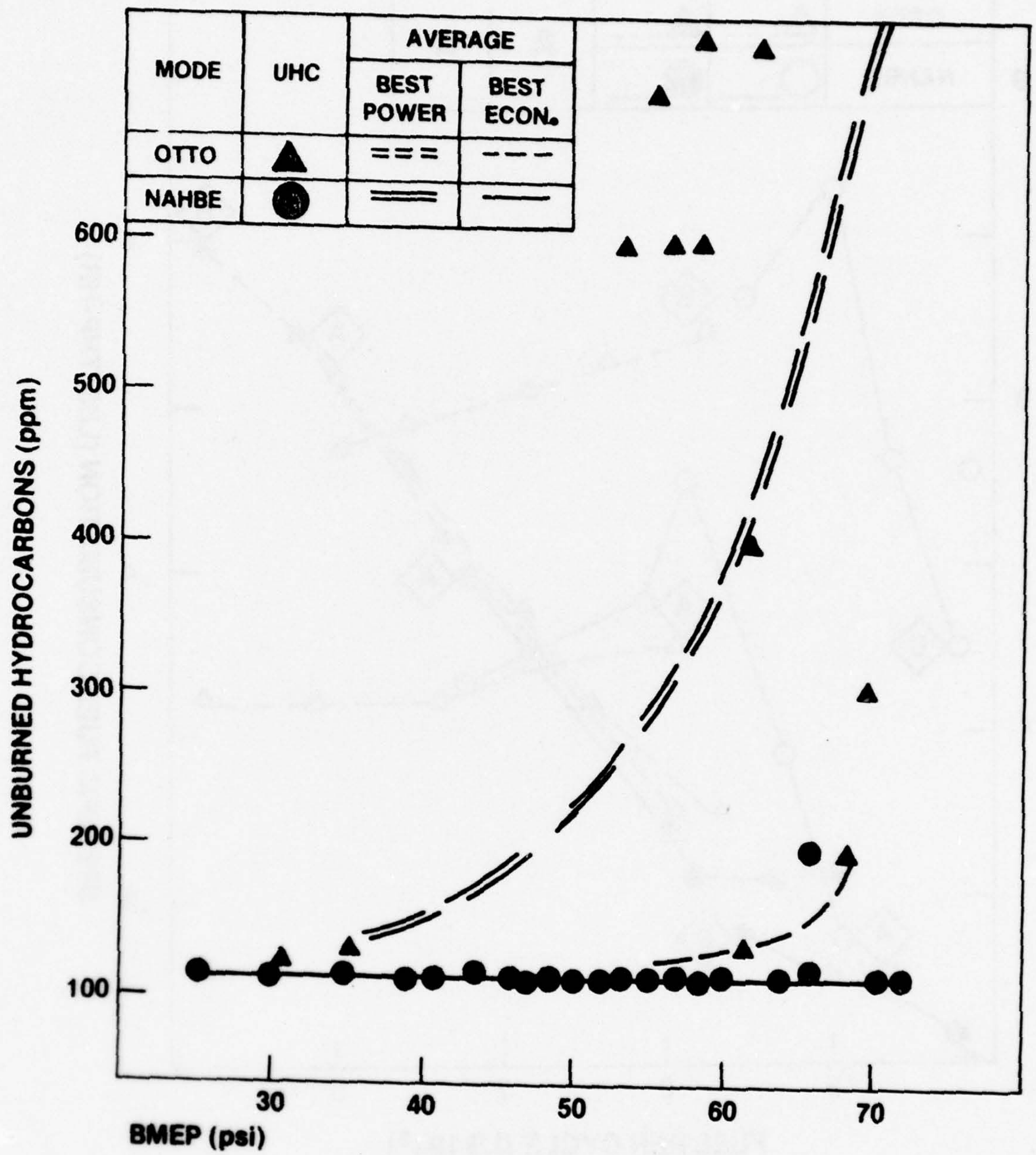

Fig. IV-3.4
CFR comparison of unburned hydrocarbons

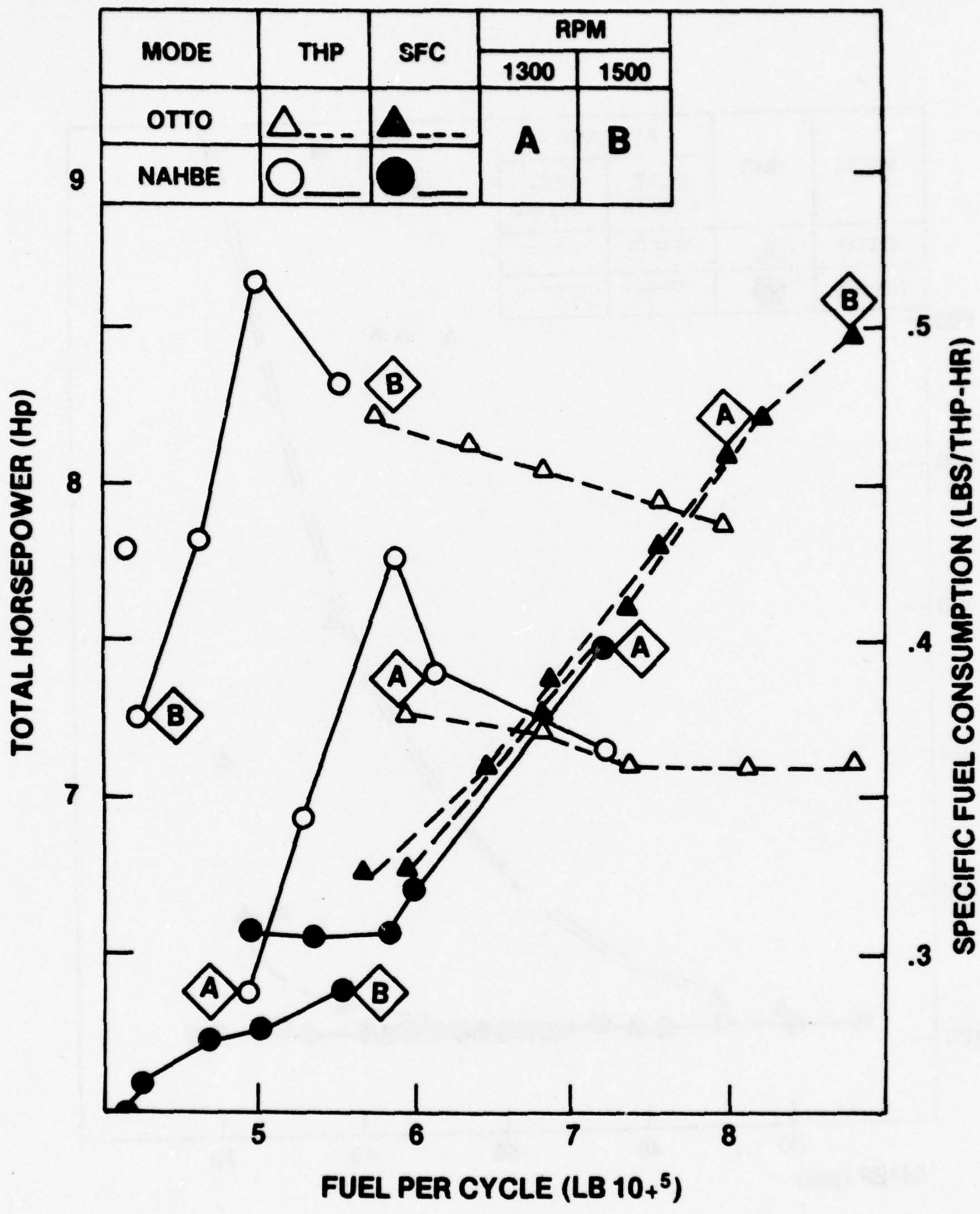

Fig. IV-3.5
CFR comparison of total output horsepower and specific fuel consumption

horsepower of 8 hp, the NAHBE consumes about 0.27 lbs of fuel per horsepower hour while the OTTO shows a consumption of about 0.41. A later figure, Fig. IV-3.11, gives the results of all tests of this series for all rpm.

In Fig. IV - 3.6 the specific fuel consumption is given versus brake horsepower. For a given output the NAHBE consumption is lower than the best OTTO performance.

f) Best Economy Comparison

At each of the five different test rpm, both the OTTO and HAHBE modes were optimized in timing; the OTTO required adjustment of fuel/air ratio as well. Presumably this gave the best engine performance at the given engine speed. Comparison of exhaust temperatures at best economy for both engine modes is given in Fig. IV-3.7. A fundamentally different process of combustion is indicated by the appreciable difference in temperature. The difference in operating range of both engines is shown in Fig. IV-3.8, with the NAHBE extending the range upward as well as to low brake outputs; the lowest output reading being essentially zero. OTTO fuel consumption does not change appreciably, even at outputs that are higher than those that can be attained with the OTTO. When output and fuel consumption is plotted versus engine speed (Fig. IV-3.9), at a given speed NAHBE output is greater thant the OTTO at lower fuel consumption.

Finally, defining thermal efficiency η in the standard manner using 2575 BTU/HP-HR and a fuel heating value of 19,000

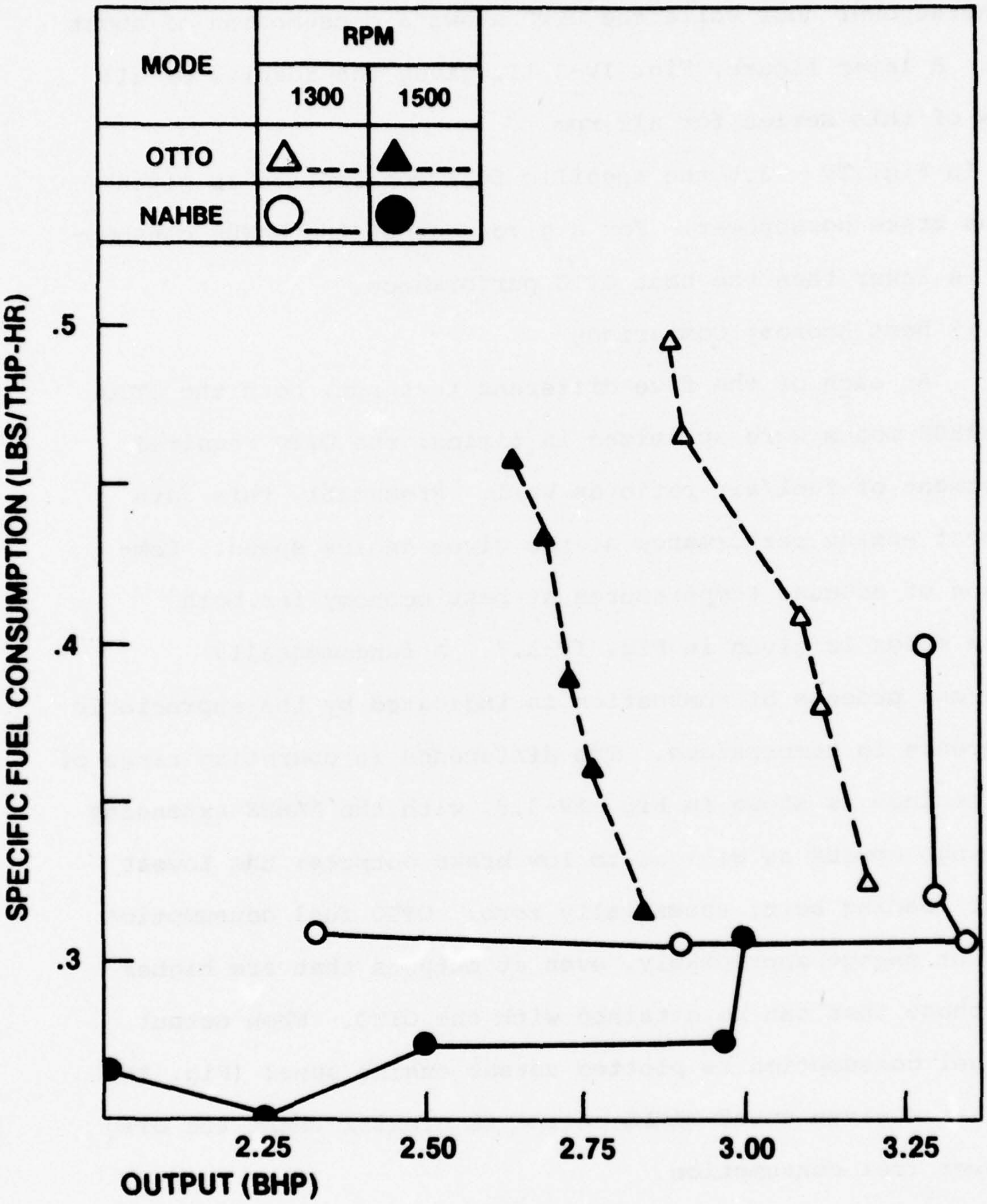

Fig. IV-3.6
CFR comparison of specific fuel consumption

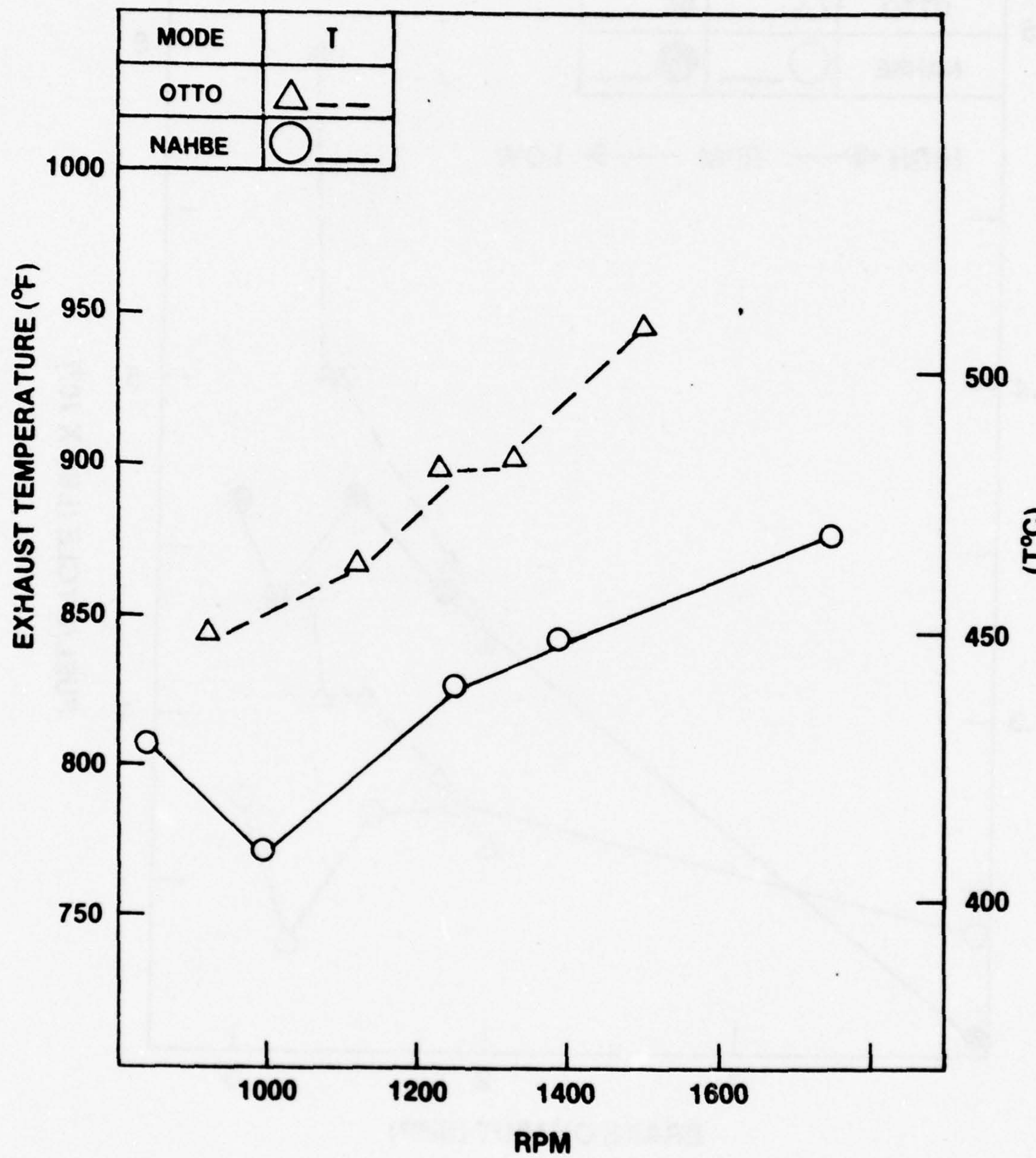

Fig. IV-3.7
Best economy comparison of exhaust gas temperature

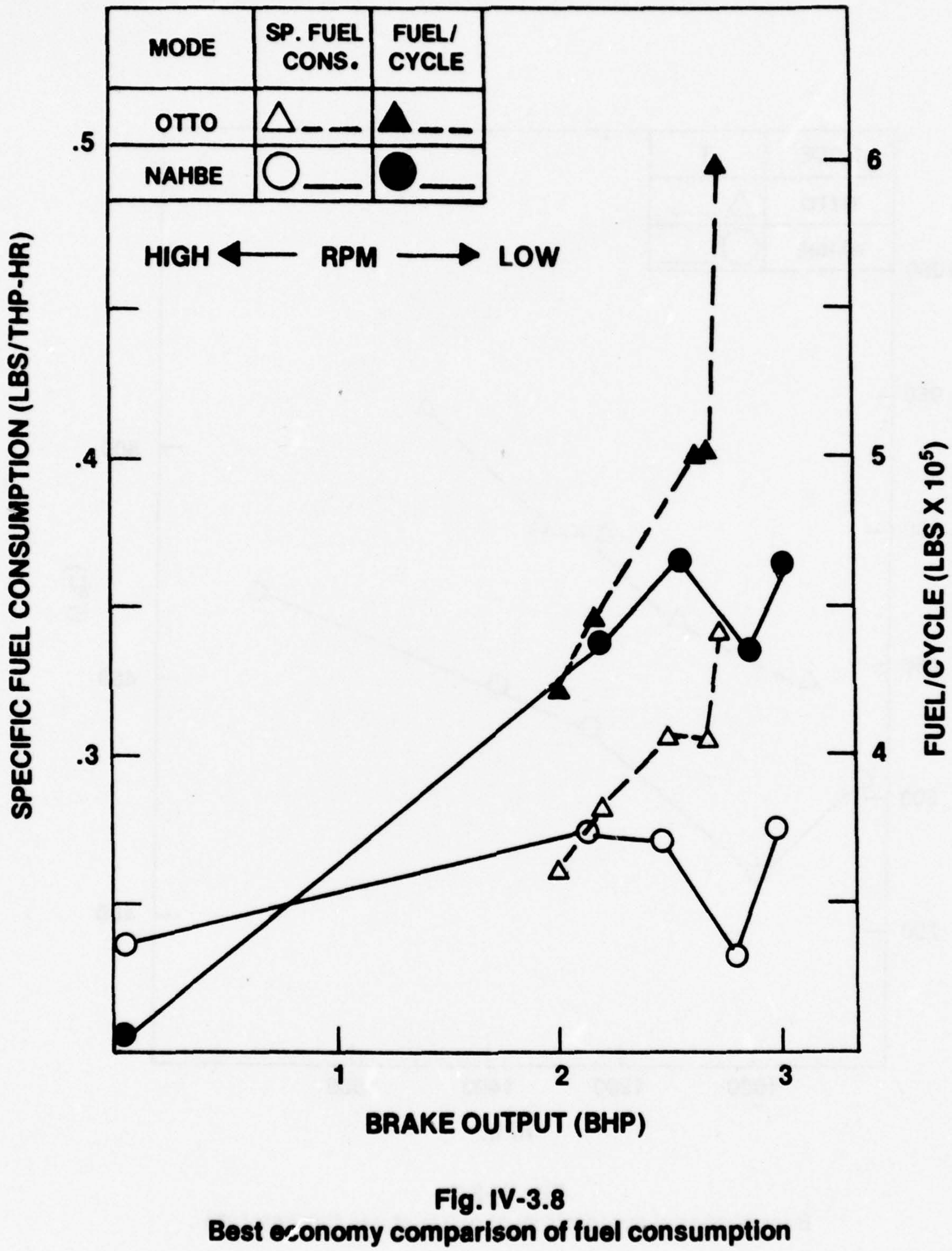

Fig. IV-3.8
Best economy comparison of fuel consumption

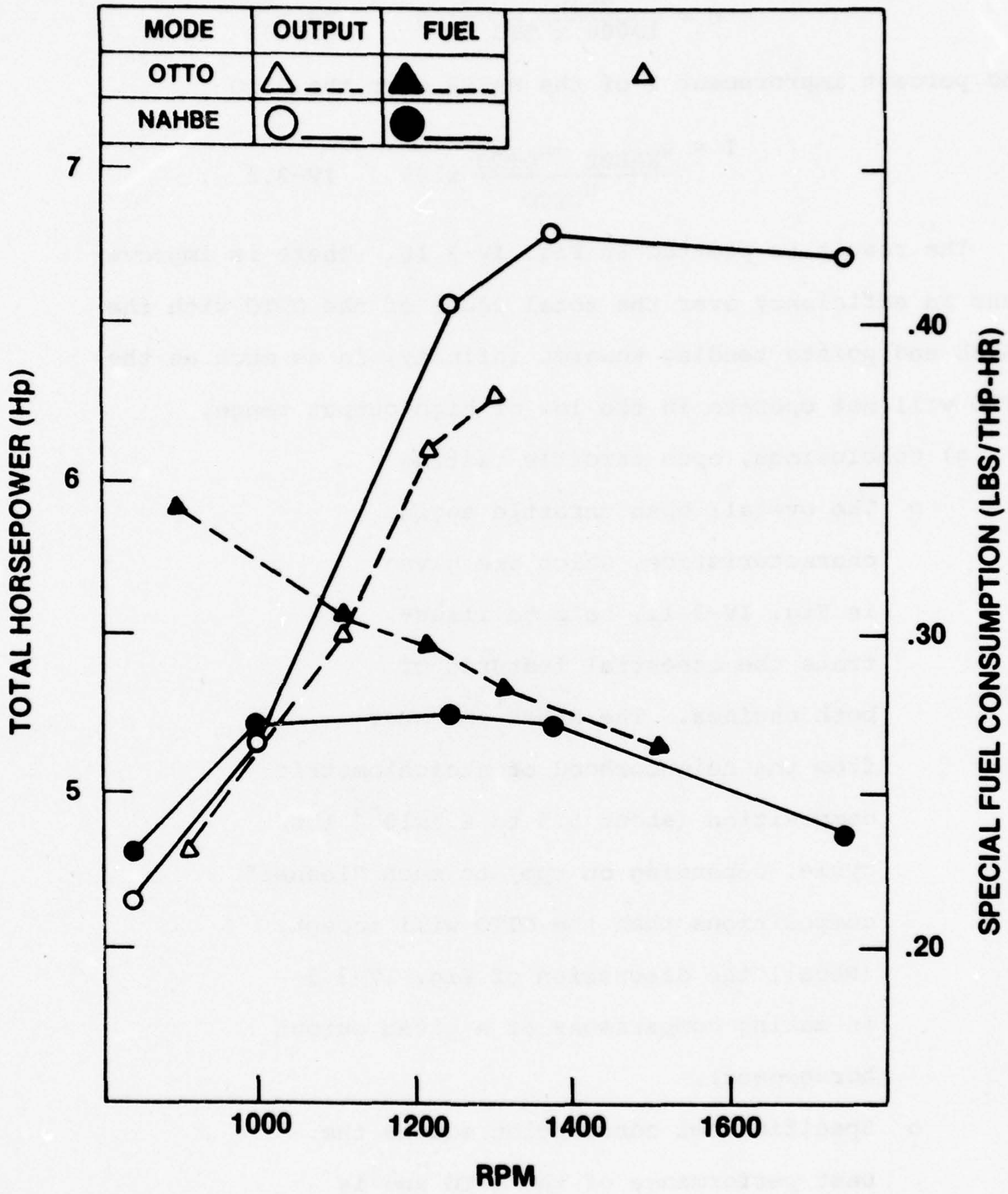

Fig. IV-3.9
Best economy comparison of total output and fuel consumption

BTU/lb gives:

$$\eta = \frac{2545}{19000 \times SFC} \times 100 \qquad \text{IV-3.1}$$

and percent improvement I of the NAHBE over the OTTO

$$I = \frac{\eta_{NAHBE} - \eta_{OTTO}}{\eta_{OTTO}} \times 100 \qquad \text{IV-3.2}$$

The result is plotted in Fig. IV-3.10. There is improvement in efficiency over the total range of the OTTO with the NAHBE end points tending towards infinity, in as much as the OTTO will not operate in the low or high output range.

g) Conclusions, open throttle testing

- o The overall open throttle engine characteristics, which are given in Fig. IV-3.11, help to illustrate the essential features of both engines. The NAHBE operates from the neighborhood of stoichiometric composition (about 5.5 to 6.5×10^{-5} lbs/cycle, depending on rpm) to much "leaner" compositions than the OTTO will accept. (Recall the discussion of Fig. IV-3.5 in making comparisons at a given output horsepower).
- o Specific fuel consumption equals the best performance of the OTTO and is generally lower.

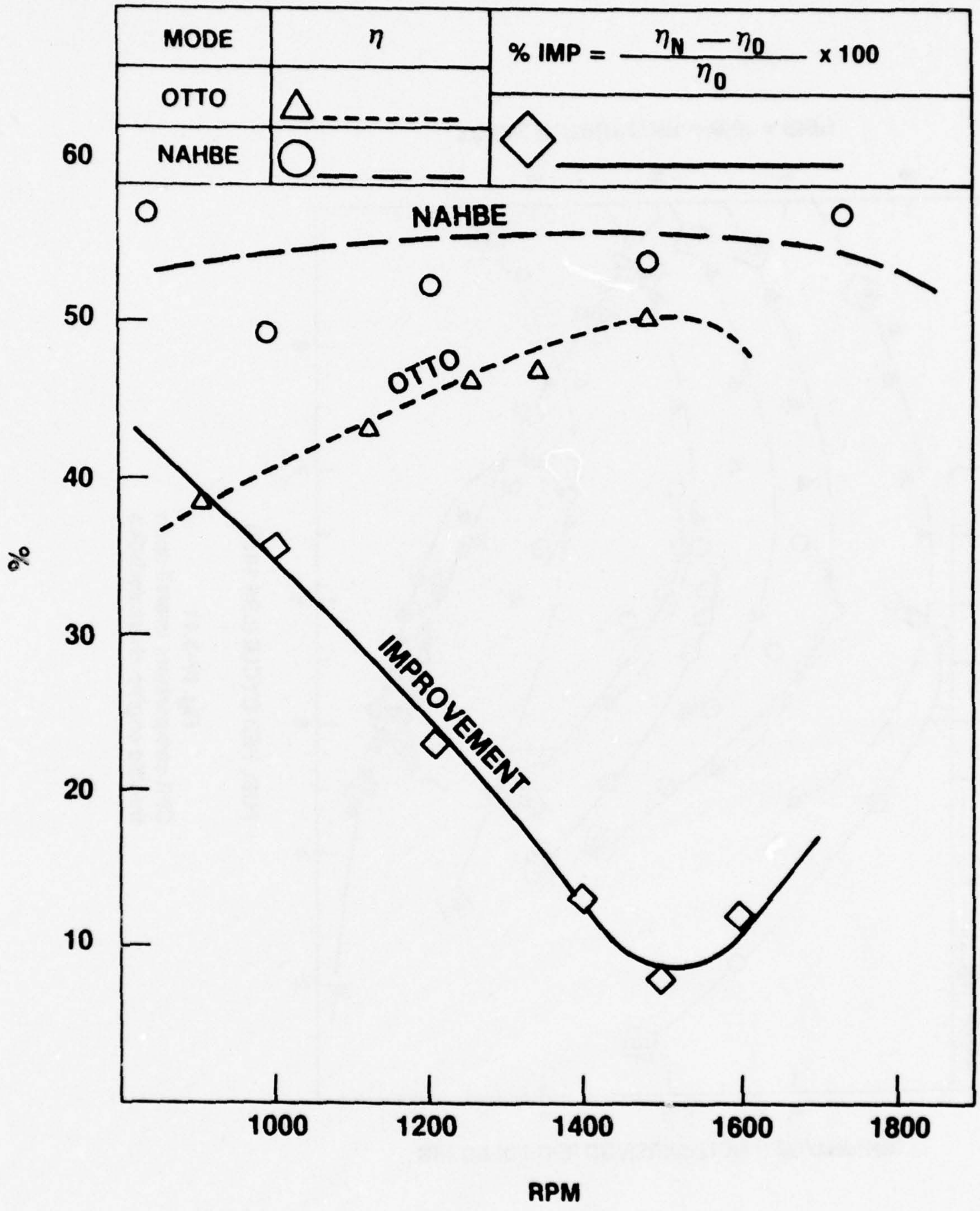

Fig. IV-3.10
Best economy comparison of efficiency and percent improvement

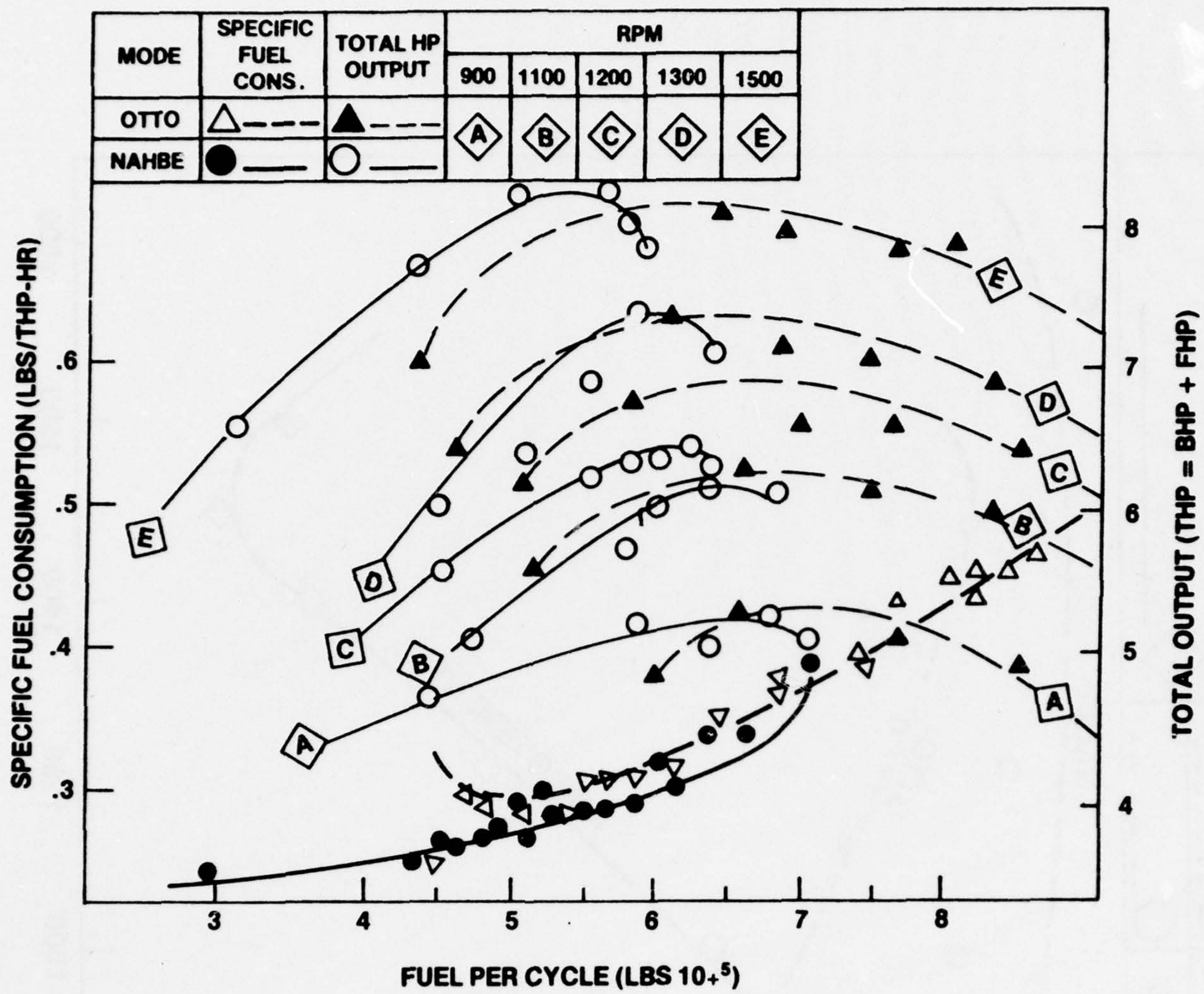

Fig. IV-3.11
CFR comparison, overall open throttle engine characteristics

- Peak pressures in the NAHBE are considerably lower than OTTO over the entire load range.
- NAHBE exhaust temperatures are proportional to the amount of fuel admitted while OTTO exhaust temperatures depend on fuel/air mixture.
- Carbon monoxide and unburned hydrocarbon emissions in the NAHBE are lower than the OTTO over the entire range of output both at best power and best economy.
- NAHBE thermal efficiency exceeds the OTTO over the entire range of the OTTO, moreover, the NAHBE will operate to both lower and higher brake loads than the OTTO.

4) Test Results, Throttled Engine Configuration

In order to compare both engine modes under other than full throttle conditions, a carburator with separate needle valves for control at idle and normal operation was fabricated and installed on the CFR engine (Fig. IV-4.1). Both needle valves were used in the OTTO mode, while only the principle valve was used in the NAHBE mode.

Tests were run at four throttle settings: minimum output, 1/3, 2/3 and full throttle. Timing was optimized for NAHBE best output while both timing and fuel were optimized for best economy in the OTTO mode. In the NAHBE mode the air was throttled only in the bypass air supply (independent of the fuel supply); a fixed flow of air through the principle venturi-jet was used to supply fuel. (See Fig. IV-4.1). Total control of metering in the NAHBE was through the principal metering needle valve. Operation in the OTTO configuration required that the bypass in Fig. IV-4.1 be closed.

The results of Figures IV-4.2 to 4.4 show that at best economy, the OTTO and NAHBE results are comparable at low loads and diverge rapidly above 2.3 horsepower. Fig. IV-4.2 shows that at best power output the NAHBE specific fuel consumption variation with throttle opening is slight: about 0.28 to 0.30 lbs/THP-HR. The OTTO variation, however, is from about 0.30 to about 0.50 lbs/THP-HR.

Fig. IV-4.4 shows the classic "best possible performance" for the OTTO. The NAHBE equals or exceeds the best possible OTTO over a wider range of operation.

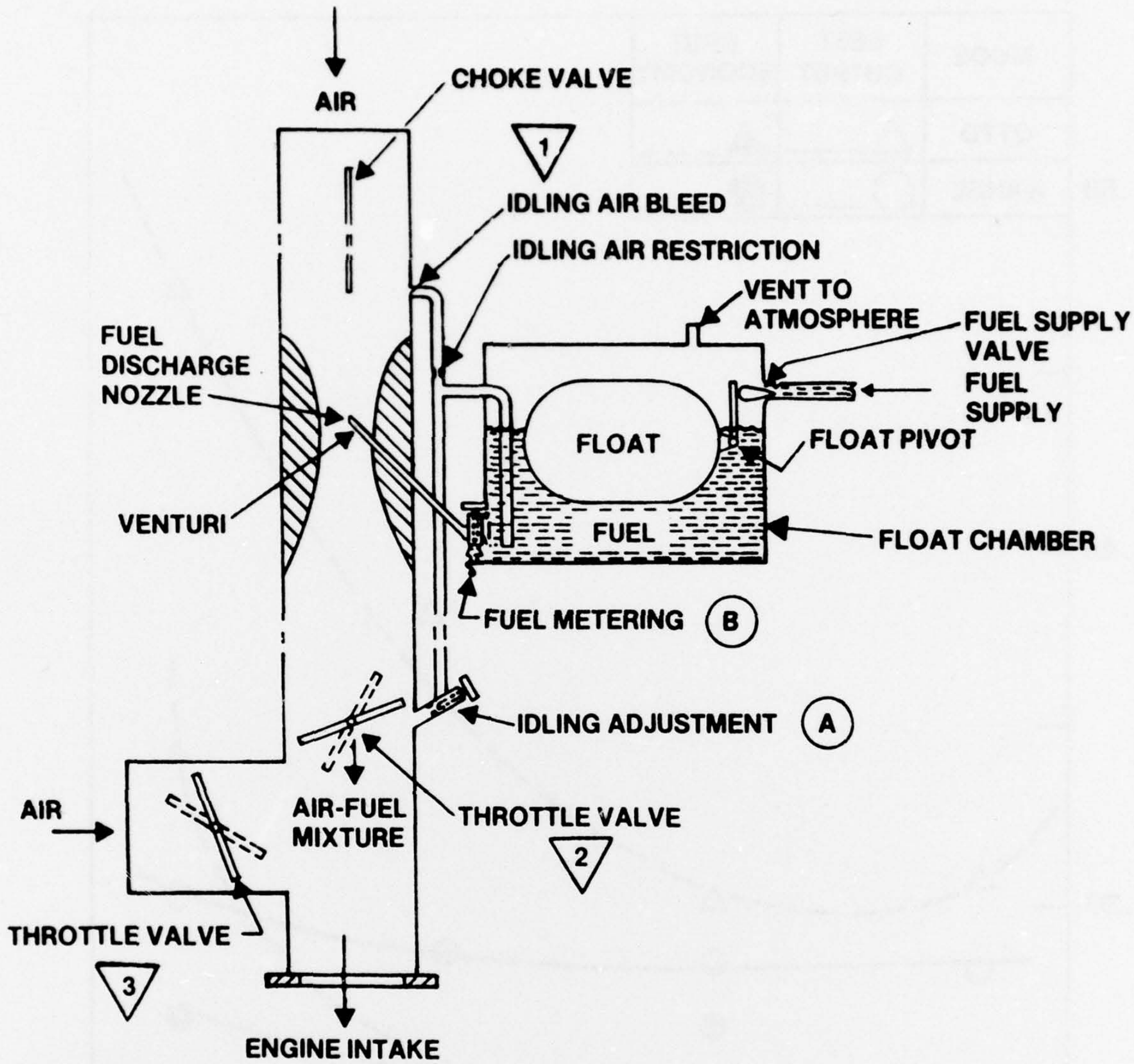

<u>OPERATION</u>

OTTO — AIR FLOW: 1—OPEN, 2—THROTTLING, 3—CLOSED.
FUEL FLOW: A—CALIBRATED BEST IDLING SETTING
B—OPTIMIZED FOR EACH THROTTLE SETTING

NAHBE — AIR FLOW: 1—CLOSED WITH ¼" DIA. BLEED HOLE
2—⅓ OPEN
3—THROTTLING
FUEL FLOW: A—CLOSED
B—VARIABLE OUTPUT METERING CONTROL

Fig. IV-4.1
NAHBE and OTTO throttling scheme

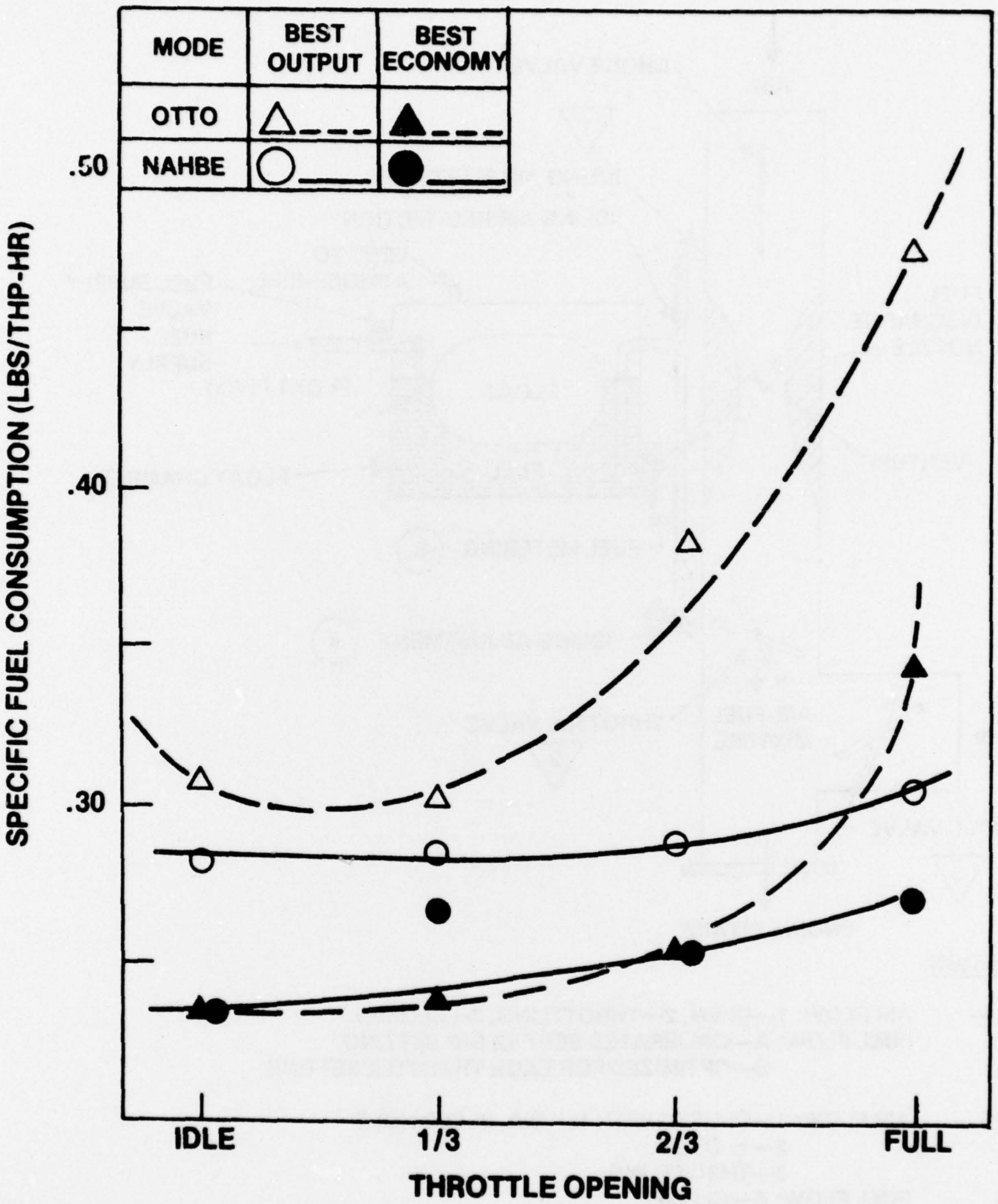

Fig IV-4.2
Throttled engine comparison of specific fuel consumption

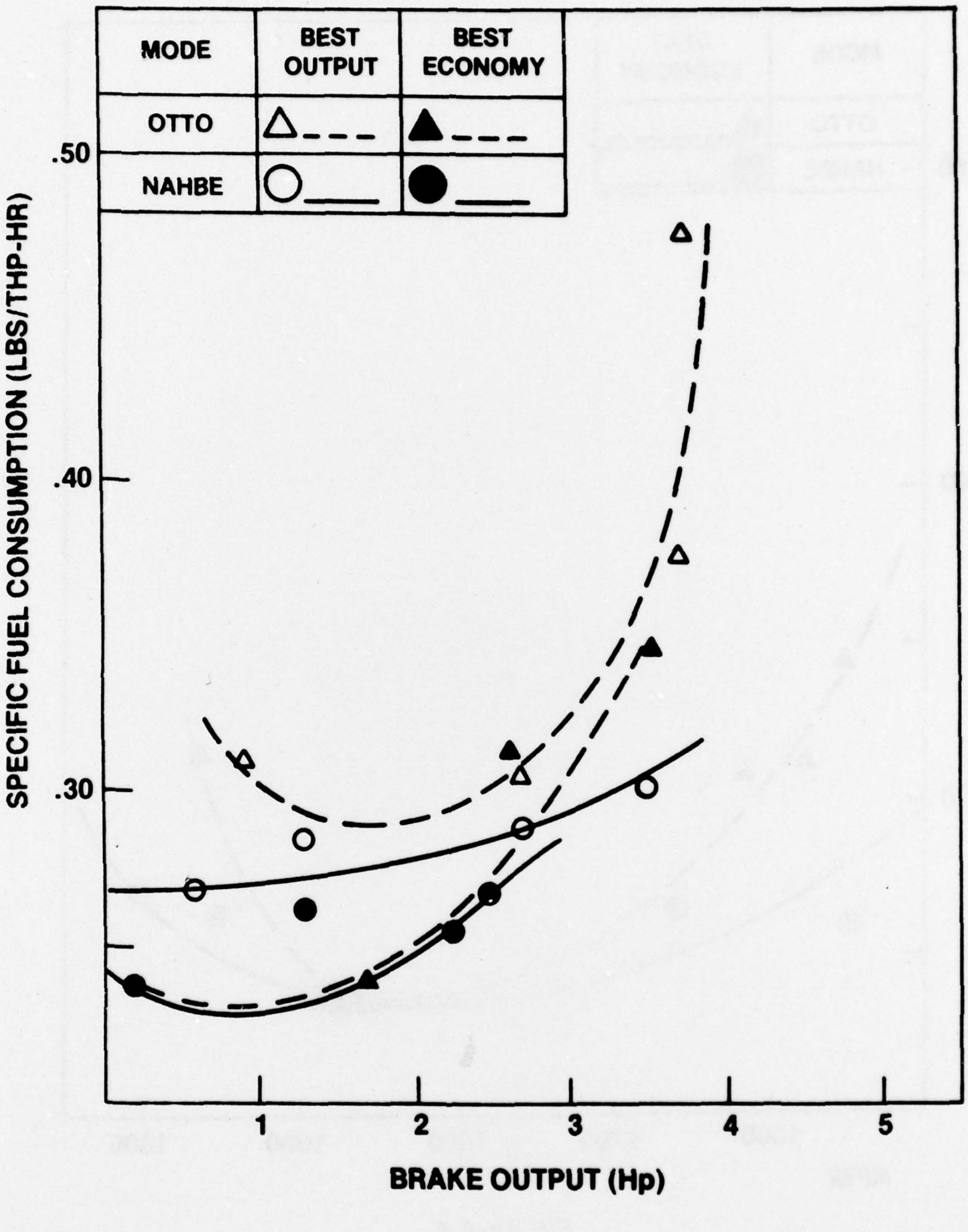

Fig. IV-4.3
Throttled engine comparison of brake output

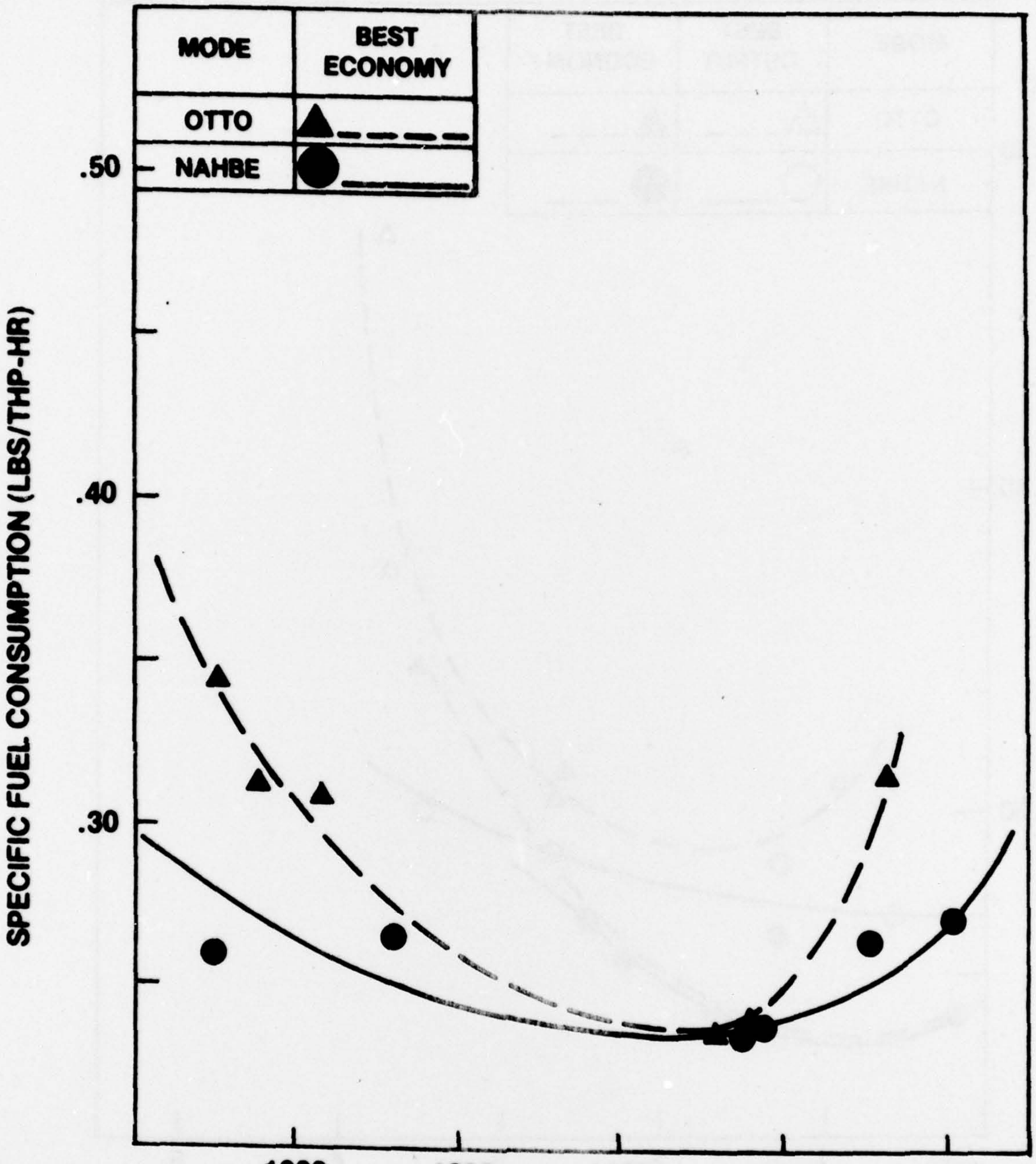

Fig. IV-4.4
Throttled engine comparison of specific fuel consumption

V. NAHBE PERFORMANCE WITH VARIABLE GEOMETRY

1. Engine Modifications for Varying Compression Ratio and Balancing Ratio

Compression ratio is the principle governing parameter in the determination of thermodynamic efficiency of the OTTO cycle. This is not the case with the combined or heat balanced cycle of the NAHBE. The balancing chamber B and clearance gap C in Fig. III - 1.1. must be considered.

In order to observe the effect of the balancing ratio $\beta = V_B/V_A$ and clearance (C) the apparatus of Figures V - 1.1 and .2 was fabricated. The pressure exchange cap assembly B, consists of a series of cover plates or caps B-1 for varying clearance (C), Fig. III- 1.1 and spacers B-2, to vary the balancing ratio β. Details are shown in Fig. V-1.2.

2. Preliminary Variable Geometry Test Results

Only two tests have been run to date; these were for compression ratios of 7 and 8 with corresponding balancing ratios of 0.5 and 0.4. Clearance was maintained constant at .075. The somewhat inconclusive test results are given in Fig. V-1.3. The wide variation in output in this series suggests experimental error requiring further confirmation.

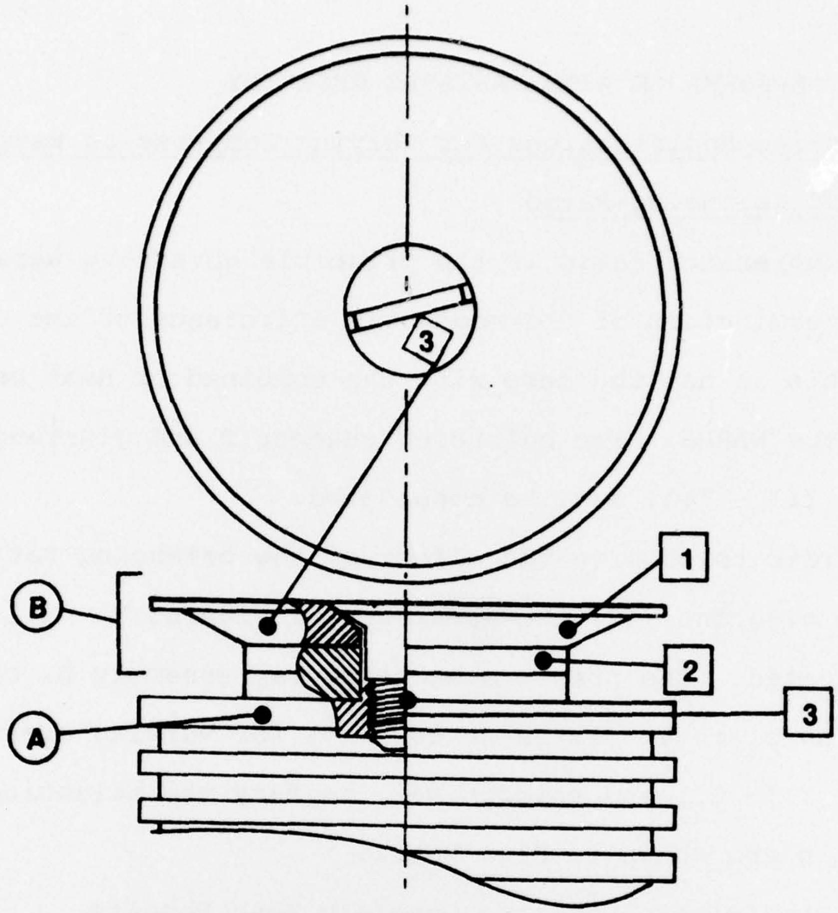

(A) OTTO STANDARD

(A) STANDARD PISTON

(B) NAHBE MODIFICATION TO PISTON

(B) PRESSURE EXCHANGE CAP

1	CAP
2	SPACER
3	BOLT

Fig. V-1.1
Piston modification for variable geometry

A

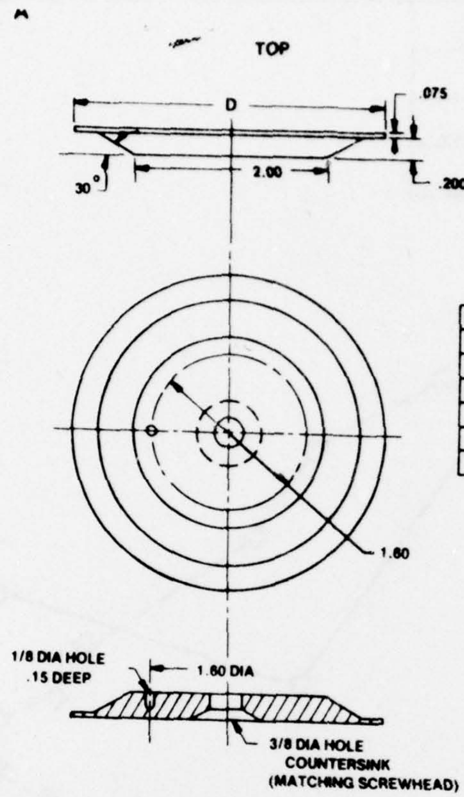

PART 010-1-NO

NO	QTY	DIM. D	GAP
1	*	3.200	.025
2		3.150	.050
3		3.100	.075
4		3.050	.100
5		3.000	.125
6		2.950	.150

MAT — STEEL
DIMENSIONS — INCHES
TOLERANCES
.XX ± .01
.XXX ± .005

B

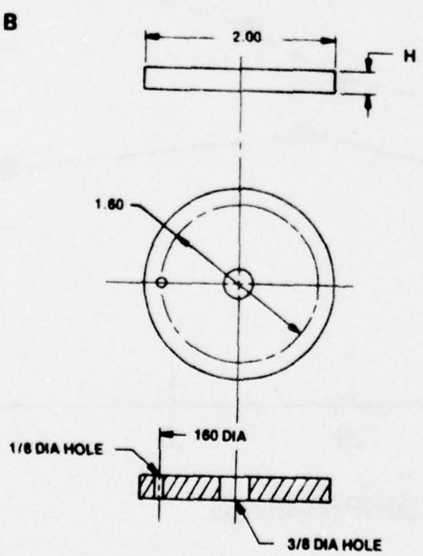

PART 010-2-NO

NO	QTY	DIM. H
1	*	.050
2		.100
3		.200
4		.400

MAT — STEEL
DIMENSIONS — INCHES
TOLERANCES
.XX ± .01
.XXX ± .005

* NOT YET DEFINED

Fig V-1.2
Details for piston modification

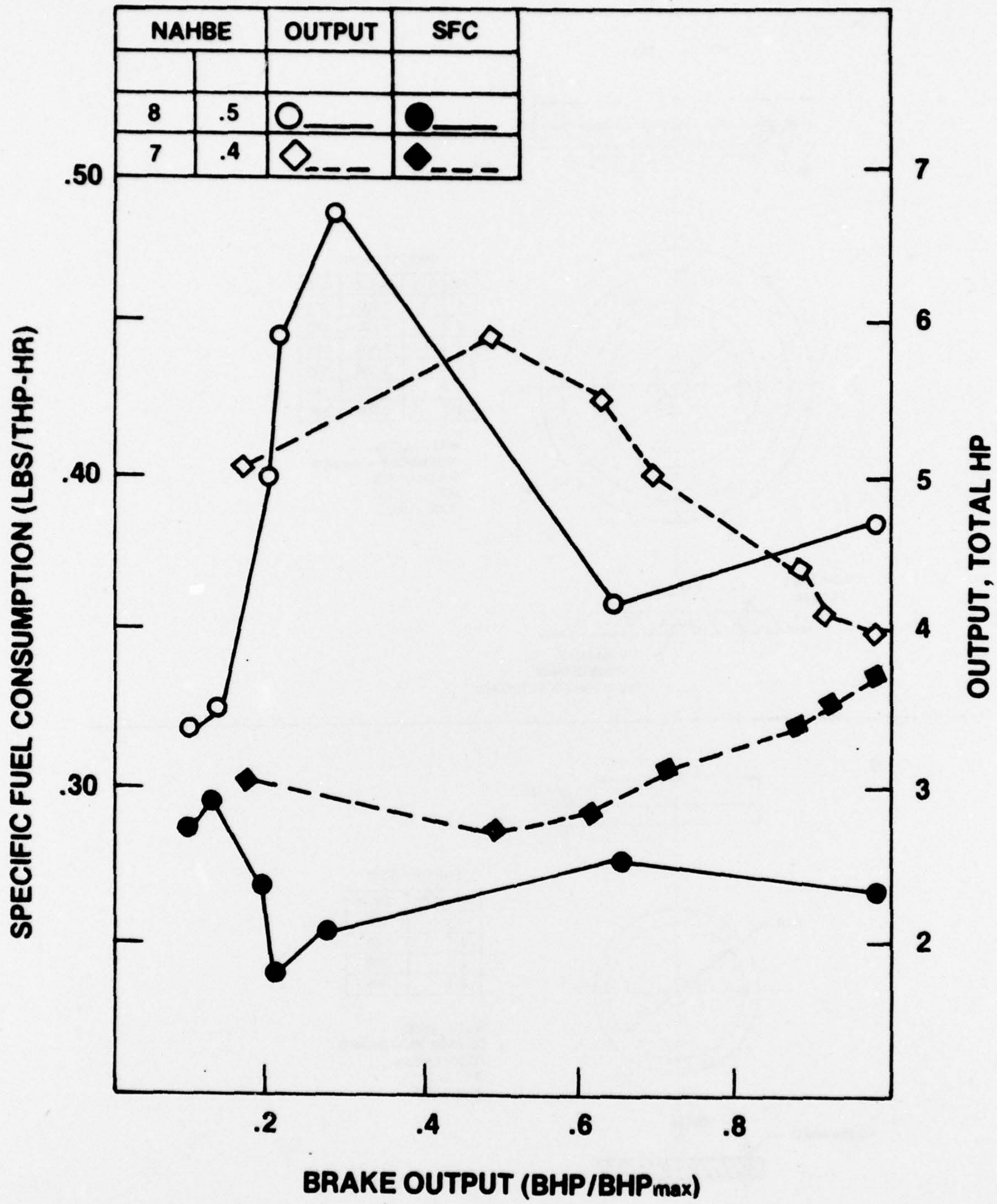

Fig V-1.3
NAHBE performance with varying compression ratio (r) and balancing ratio (β)

VI. NAHBE COMPRESSION IGNITION BEHAVIOR

1. Preliminary Results

During engine testing it was observed that smooth operation of the CFR was possible in the NAHBE mode with compression ignition of regular gasoline fuel. This engine mode does not have the serious knock behavior of the OTTO, and when knock occurs the accompanying pressure increase is moderate. Compression ignition (CI) operation with regular gasoline is given in Fig. VI-1.1 at a compression ratio of 8.0 and balancing ratio of 0.5. Operation is smooth and controllable over the full range. For comparison spark ignition (SI) behavior of both modes is also given.

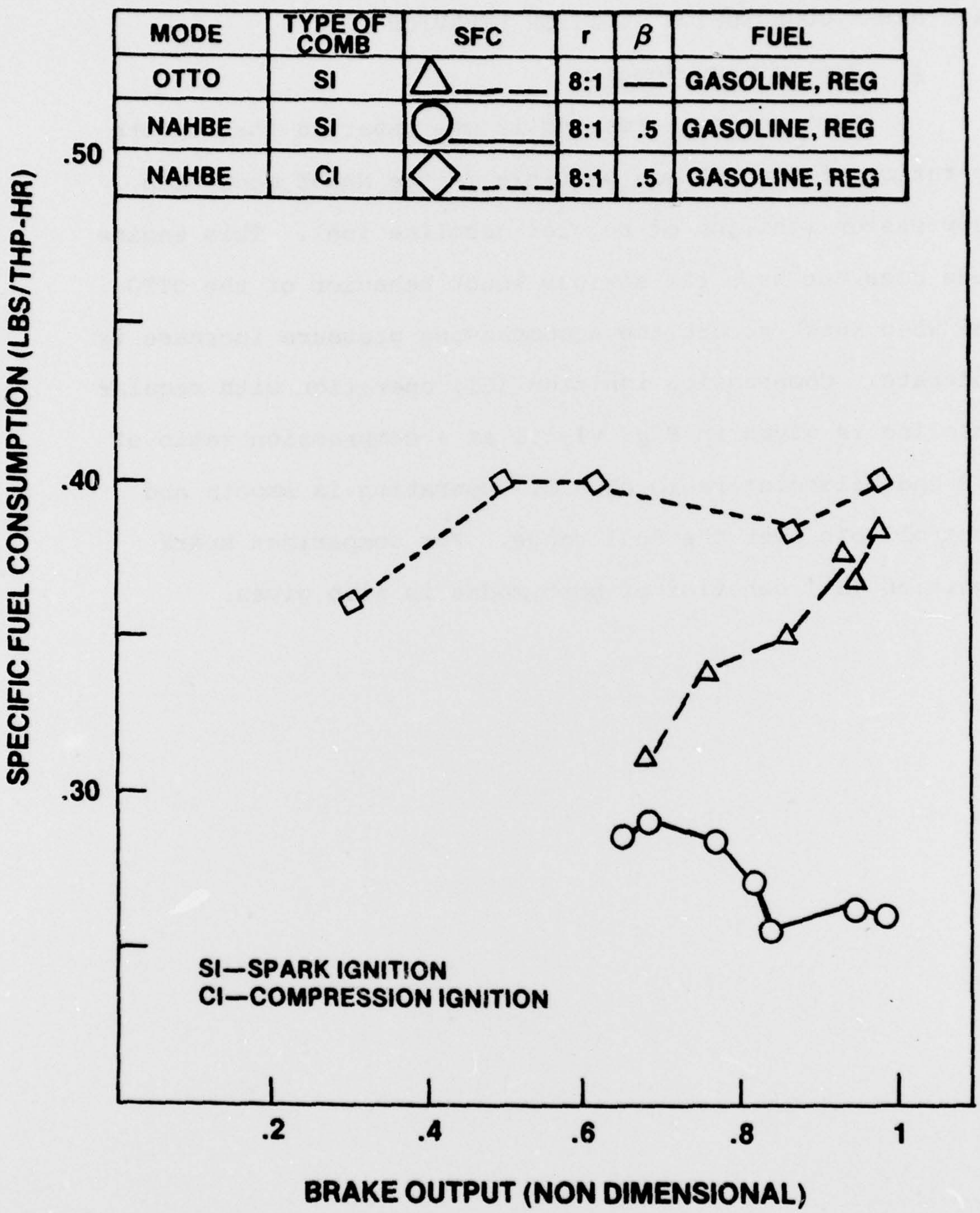

Fig VI-1.1
NAHBE compression ignition behavior with gasoline, comparison with OTTO.

VII. FUTURE RESEARCH

Research is currently underway to gain more understanding of the phenomena of combustion with pressure exchange. A glass walled engine is currently being modified for optical studies as well as piezoelectric transducer studies of the pressure within a balancing chamber. Computer simulation of an equilibrium reaction combustion model is also in progress. Parametric variation of CFR balancing chamber volume, clearance gap and compression ratio is in progress, for both compression and spark ignition behavior. An analytical investigation from the point of view of non-steady gas dynamics has also been initiated. Dynamometer and road testing of a four-cylinder engine is currently in progress.

Further investigation into multi-fuel performance, 2 cycle behavior and adaptation to the rotary engines are in order.

References

1. Blaser, R. R., S. T. Hsu, and R. A. Granger, The Controlled Heat Balanced Cycle, APS Annual Meeting, Pasadena, Calif., Nov. 1974.

2. Foa, J. V., Elements of Flight Propulsion, John Wiley, New York, 1960.

3. Rudinger, G., Wave Diagrams for Nonsteady Flow, Van Nostrand, New York, 1955.

78